


Einstein-Laub and Lorentz optical force densities with a planar interfaceAdam W. Behnke , Thomas J. Pollei , and Kevin J. Webb **School of Electrical and Computer Engineering, Purdue University, West Lafayette, Indiana 47907, USA* (Received 4 April 2023; revised 12 June 2023; accepted 7 July 2023; published 11 September 2023)

A definitive theory for the optical or electromagnetic force density in condensed matter has remained elusive. Integral in such a theory is how material interfaces are treated. To build collective understanding, a general planar interface situation between vacuum and a semi-infinite, nonmagnetizable material medium is studied analytically using two electromagnetic force density formulations and an obliquely incident, p -polarized plane wave impinging on the material surface. A form of the Lorentz electromagnetic force density formulation and the Einstein-Laub electromagnetic force density are shown to both predict a total pressure that agrees with that predicted by the so-called “Maxwell-Bartoli” expression modified for oblique incidence. However, the two formulations present different distributions of the total force between the surface and bulk of the material. The quantification of this difference and of the implied outward surface pressure for this broadly applicable field geometry offers opportunities for the experimental determination of a force density theory that accurately predicts experiment.

DOI: [10.1103/PhysRevA.108.033708](https://doi.org/10.1103/PhysRevA.108.033708)**I. INTRODUCTION**

Understanding the interaction between electromagnetic fields and condensed matter is becoming increasingly important in modern physics. Despite years of theoretical investigation [1–4] and experimental efforts [5–8], there still remain open questions relating to how one should calculate a force on condensed matter given a distribution of electromagnetic quantities. Two formulations that have been studied [9,10] include a particular interpretation of the well-known Lorentz formulation in charge-neutral material, and the Einstein-Laub formulation, first proposed in Ref. [4]. To treat the fundamental physics of motion involving photons requires concomitant understanding of the momentum exchange between light and matter, hence the very great interest in a theory that can be used to describe the relevant physics and predict experimental results. One starting point for a theory describing the optical force on an object is to consider the total force as the spatial integral of a spatially and temporally dependent force density. This invariably involves dealing with interfaces as part of this formalism.

A review paper has provided a compilation of related concepts and experiments [11]. One basic issue has been how to interpret the photon momentum in a background material, the so-called Abraham-Minkowski question [12–16]. In applications, calibration for optical forces on small particles [17] is relevant in the use of optical tweezers [18,19], and optically trapped atoms have long been important in metrology [20]. To predict how matter moves, the internal forces must be accessed [21], as has been investigated for metamaterials

[22]. Also, a theoretical study of the optical force on “bilayer \mathcal{PT} -symmetric structures” (structures having parity-time symmetry), in this case a bilayer slab where one side has loss and the other gain, has indicated the asymmetric behavior of the optical force under illumination from both directions [23]. This and other work motivates the understanding of key optical force problems.

To provide more opportunities for experimental investigation, we present an analytical investigation of multiple formulations for the pressure due to radiation. We consider the simple case of a plane wave incident on the planar surface of a material (which may or may not be lossy), given the local planar approximation’s usefulness and the relevance to investigations of electromagnetic interactions at material surfaces [24,25]. Through the analysis of this simple field geometry, we develop several key results that unify widely applied models. We demonstrate that the Maxwell-Bartoli expression for normal incidence follows directly from the evaluation of the Maxwell stress tensor in the case of counterpropagating plane waves. For plane waves at oblique incidence with p polarization (having electric field in the plane of incidence, defined by the incident field wave vector and the normal to the surface), we show that an interpretation of the Lorentz formulation (as previously applied to this field geometry [26]) and the Einstein-Laub formulation agree in the total predicted pressure when the force density is integrated in the bulk and across the surface of the material, where the expectation of agreement in total force between the two formulations has been put forward previously [27]. Moreover, we demonstrate analytically that both formulations agree exactly with a form of the Maxwell-Bartoli expression modified for oblique incidence. Finally, although the formulations agree in the predicted total pressure, their predictions of the distribution of electromagnetic forces between the surface and bulk of the material are shown to differ, and this difference is quantified. The current

*Corresponding author: webb@purdue.edu; Supported by the Air Force Office of Scientific Research, the Army Research Office, and the National Science Foundation.

understanding of how electromagnetic forces are distributed throughout condensed matter would continue to benefit from further experimental investigation, and this analysis provides a numerical difference between the predictions of the two formulations under study against which empirical evidence can be compared.

Section II provides a brief background on the interesting history of the so-called ‘‘Maxwell-Bartoli’’ expression for radiation pressure. Section III describes the material geometry and electromagnetic field solution under study in the oblique incidence situation of interest. The Lorentz and Einstein-Laub force density formulations are applied to the field solution in Secs. IV and V, both of which are shown analytically to predict the same total pressure as the Maxwell-Bartoli expression in Sec. VI, despite differing in the predicted force densities at the surface and in the bulk of the material. The derived expressions for pressure are applied to several situations of theoretical and experimental interest in Sec. VII. The results presented and their relevance are summarized in Sec. VIII.

II. MAXWELL-BARTOLI EXPRESSION BACKGROUND

J. C. Maxwell [28] gave an electromagnetic field-based line of reasoning in the case of a plane wave that predicted the existence of a radiation pressure ‘‘in the direction normal to the waves, and numerically equal to the energy in unit of volume’’ [29]. Using this, he also gave a numerical prediction of the pressure exerted by sunlight normally incident on a material as ‘‘mean pressure on a square foot is 0.000000882 of a pound weight’’ [29]. Around the same time, A. Bartoli gave an argument based on the laws of thermodynamics for the existence of a pressure exerted by any stream of energy in space [2,3], considering in particular ‘‘radiant heat.’’ The history of Bartoli’s publications and their role in the discourse surrounding the existence of radiation pressure is a substantive topic in and of itself, as discussed in Ref. [30]. In Bartoli’s theoretical investigation is an analytical expression which predicts a pressure on a perfectly reflecting surface equal to twice the energy delivered by the energy stream per unit area per unit time, divided by the stream’s propagation speed. He too gave a numerical prediction; his for sunlight impinging normally on a perfectly reflecting surface. His prediction was given as 0.84 milligrams of force per square meter. Upon converting the units of Maxwell’s numerical prediction (using modern conversion factors of 1 ft = 0.3048 m and 1 lbf = 453592.37 mgf), we find that Maxwell’s prediction is equivalent to approximately 0.4306 milligrams-force per square meter; about half of Bartoli’s prediction, implying that Maxwell’s would hold for an absorbing surface. These two investigations laid theoretical groundwork for quantifying the pressure due to radiation.

Early experimental investigations of radiation pressure by Nichols and Hull [31] and Lebedew [6] compared their experimental results with theory by citing what they called the Maxwell-Bartoli formula, written originally in the previously referenced works as

$$p = \frac{E(1 + \rho)}{V}, \quad (1)$$

where p is the radiation pressure, E is interpreted as the intensity of the beam (energy delivered by the beam per unit

area per unit time), V is the propagation velocity of the beam, and ρ is the intensity reflection coefficient of the medium. It appears to be implied that any energy that is transmitted to the medium is subsequently absorbed. It is also worth noting that, in the case of a single plane wave, the intensity (E) in free space is equal to its energy volume density times the speed of light (V). It follows that the quotient E/V is equivalent to ‘‘the energy in unit of volume’’ of the wave, as in Maxwell’s phrasing. As can be seen, the expression (1) linearly interpolates in reflected power between the numerical predictions of Maxwell for a perfectly absorbing medium, and Bartoli’s for a perfectly reflecting medium.

Equation (1) has been adapted to more modern notation, as well as for oblique angle of incidence, as [32]

$$P_{\text{MB}} = \frac{|\langle \mathbf{S}_i \rangle|}{c} (1 + |\Gamma|^2) \cos^2 \theta_i, \quad (2)$$

where $|\langle \mathbf{S}_i \rangle|$ is the time-averaged magnitude of the incident wave’s Poynting vector (where $\mathbf{S}_i = \mathbf{E}_i \times \mathbf{H}_i$, with \mathbf{E}_i and \mathbf{H}_i as the incident electric and magnetic fields, respectively), equal to the time-averaged flux of electromagnetic power per unit area, with the area measured in the plane perpendicular to the direction of propagation; c is the speed of light in vacuum; $|\Gamma|^2$ is the power reflection coefficient; and θ_i is the angle of incidence referenced to the surface normal. The factor of the squared cosine of the angle of incidence has been included previously [26,32,33], and can be thought of as accounting for both the change in direction of the incident electromagnetic momentum density, as well as the change in the direction of the flow of that same momentum density, as the angle of incidence changes. This momentum density with a direction of flow can be considered as either momentum carried by fields or, in terms of quantized momentum, as photon flux. We note that for both (1) and (2), the assumption of a defined direction of propagation implicitly assumes a single-plane-wave geometry. The expression given in (2) in the case of normal incidence can be shown to result from evaluation of the Maxwell stress tensor, as is done in Appendix A.

In the case of a slab of finite thickness, where all photons are not either absorbed or reflected and some are transmitted, the expressions for semi-infinite media in (1) and (2) do not hold. A variant has been derived from stress tensor principles for a finite slab, including transmission, in the case of a normally incident plane wave (see the Appendix of Ref. [23]).

III. FIELD SOLUTION AND MATERIAL GEOMETRY FOR p -POLARIZED OBLIQUELY INCIDENT RADIATION

We now turn our attention to the case of monochromatic, p -polarized plane-wave radiation obliquely incident on a planar interface with a semi-infinite, isotropic, nonmagnetic, lossy material, as illustrated in Fig. 1. The fields can be written using projected impedances, resulting in the field solutions using an $\exp(i\omega t)$ time convention:

$$\mathbf{E} = H_{0i} e^{-ik_x x} [\hat{\mathbf{z}} Z_{z0} (e^{-ik_{iz} z} - \Gamma_h e^{ik_{iz} z}) - \hat{\mathbf{z}} Z_{x0} (e^{-ik_{iz} z} + \Gamma_h e^{ik_{iz} z})], \quad (3a)$$

$$\mathbf{H} = \hat{\mathbf{y}} H_{0i} e^{-ik_x x} [e^{-ik_{iz} z} + \Gamma_h e^{ik_{iz} z}], \quad (3b)$$

for $z < 0$ (in free space), where $Z_{z0} = E_{xi}/H_{yi} = k_{iz}/(\omega\epsilon_0) = \eta_0 \cos \theta_i$ is the z -projected wave impedance in free space

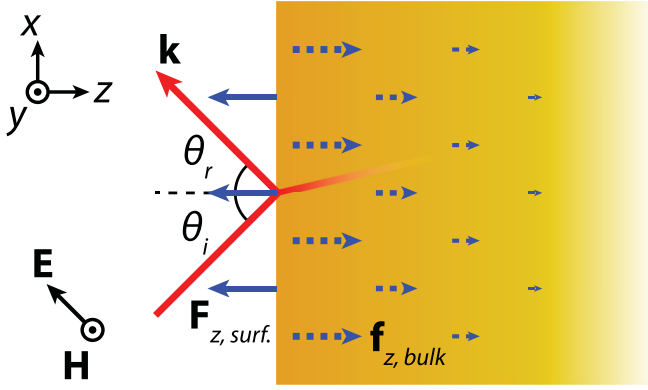


FIG. 1. The geometry of material, fields, and forces under study in Secs. III–V. *P*-polarized radiation is obliquely incident on a lossy material, with the interface modeled using the piecewise-constant model [24], which simply models the interface as an abrupt change in material parameters at $z = 0$. Forces are shown as blue arrows, with solid arrows indicating electromagnetic forces confined to the surface and dashed indicating force densities in the bulk of the material. The decreasing dashed arrow size indicates the exponentially diminishing force density into the material.

and $Z_{x0} = -E_{zi}/H_{yi} = k_x/(\omega\epsilon_0)$ is the x -projected wave impedance in free space. Then, for $z > 0$ (in the material), the phase-match condition and continuity of tangential fields are satisfied by the fields

$$\mathbf{E} = H_{0i}T_h e^{-i(k_x x + k_{tz} z)} (\hat{\mathbf{x}}Z_{zm} - \hat{\mathbf{z}}Z_{xm}), \quad (4a)$$

$$\mathbf{H} = \hat{\mathbf{y}}H_{0i}T_h e^{-i(k_x x + k_{tz} z)}, \quad (4b)$$

where $Z_{zm} = E_{zt}/H_{yt} = k_{tz}\eta/k = k_{tz}/(\omega\epsilon) = \eta_0(\epsilon_r - \sin^2\theta_i)^{1/2}/\epsilon_r$ is the z -projected wave impedance in the material and $Z_{xm} = E_{xt}/H_{yt} = k_x/(\omega\epsilon)$ is the x -projected wave impedance. Here, H_{0i} is the amplitude of the incident magnetic field, Γ_h is the magnetic-field reflection coefficient (now defined as H_{yr}/H_{yi} , with H_{yi} and H_{yr} being the complex incident and reflected y -directed magnetic-field amplitudes, respectively), $T_h = 1 + \Gamma_h$ is the magnetic-field transmission coefficient [resulting from the required continuity of the tangential magnetic field across the interface seen in (3b) and (4b)], $k_0 = \omega\sqrt{\mu_0\epsilon_0}$ is the free-space wave number, $\eta_0 = \sqrt{\mu_0/\epsilon_0}$ is the free-space wave impedance, $\epsilon_r = \epsilon'_r + i\epsilon''_r = 1 + \chi_E$ is the complex relative dielectric constant of the lossy medium, χ_E is the complex electric susceptibility of the medium, $\epsilon = \epsilon_r\epsilon_0$ is the complex permittivity of the medium, $k_x = k_0 \sin\theta_i$ is the x component of the wave vector in both free space and the medium (due to the phase-match condition), $k_{tz} = k_0 \cos\theta_i$ is the z -component of the wave vector in free space, $k = k_0\sqrt{\epsilon_r}$ is the complex wave number in the material, $k_{tz} = (k^2 - k_x^2)^{1/2}$ is the z -directed complex wave number in the material of the transmitted wave (from the dispersion relation), and $\eta = \eta_0/\sqrt{\epsilon_r}$ is the complex wave impedance in the material. The magnetic-field reflection coefficient Γ_h is formed as

$$\Gamma_h = \frac{Z_{z0} - Z_{zm}}{Z_{zm} + Z_{z0}}. \quad (5)$$

From $T_h = 1 + \Gamma_h$, it also follows that

$$T_h = \frac{2Z_{z0}}{Z_{zm} + Z_{z0}}. \quad (6)$$

Equations (3a), (3b), (4a), and (4b), with (5) and (6), will be used throughout this paper.

IV. LORENTZ PRESSURE EVALUATION

We now introduce the first force density formulation of interest, whose name and precise definition here in the context of condensed macroscopic media are worthy of some explanation. Known commonly as the ‘‘Lorentz force,’’ it can be expressed in terms of the force on a point charge moving in an electromagnetic field distribution. It is given in one of its common forms by [34]

$$\mathbf{F}_L = q(\mathbf{E} + \mathbf{v} \times \mathbf{B}), \quad (7)$$

where \mathbf{F}_L is the electromagnetic force exerted on a point charge q moving with velocity \mathbf{v} , and \mathbf{B} is the magnetic flux density (also called magnetic induction). This form has been claimed [35] to be attributed to Lorentz due to an 1895 publication [36–38] of his in which he writes the total electromagnetic force on a charged particle due to both electric and magnetic fields. A force expression of this form provides a definition of the fields \mathbf{E} and \mathbf{B} [39].

Concerning the expression’s history, it is worthy of note that Lorentz in fact wrote a form of this expression in terms of a continuum of charge density even earlier, in 1892 [40,41] [similar to (8) below]. The forms of the forces on a charge due to the individual fields were at that time not new, however. As noted in Ref. [42], Thompson theoretically deduced the form of the force on a charge moving through a magnetic field in 1881 [43], and Heaviside subsequently corrected an erroneous factor of one half in 1889 [44,45]. Even before that, it can be argued that Maxwell effectively deduced this general form himself in 1861 [46], by including the magnetic field’s contribution to the electromotive force in a moving body.

Separate from the history of the name of the expression, one can still occasionally find in more recent literature differing approaches to applying this expression inside charge-neutral materials [47], which can lead to some ambiguity in the term’s meaning. For this reason, we review the formalism used here.

Equation (7) can be written based on volume densities as [39,48]

$$\mathbf{f}_L = \rho\mathbf{E} + \mathbf{J} \times \mathbf{B}, \quad (8)$$

where \mathbf{f}_L is the Lorentz force volume density, ρ is the charge volume density, and \mathbf{J} is the current density. For a system of free charges and currents in free space, it can be shown through manipulation of (8) using Maxwell’s equations that \mathbf{f}_L is related to the Maxwell stress tensor by the momentum conservation equation [48]

$$\mathbf{f}_L = -\left(\nabla \cdot \mathbf{T}_M + \frac{\partial \mathbf{g}}{\partial t}\right), \quad (9)$$

where the Maxwell stress tensor \mathbf{T}_M has the form [48,49]

$$\mathbf{T}_M = \frac{1}{2}(\epsilon_0\mathbf{E} \cdot \mathbf{E} + \mu_0^{-1}\mathbf{B} \cdot \mathbf{B})\mathbf{I} - \epsilon_0\mathbf{E}\mathbf{E} - \mu_0^{-1}\mathbf{B}\mathbf{B}, \quad (10)$$

with \mathbf{I} the identity tensor and the electromagnetic momentum density \mathbf{g} in free space having the form [48]

$$\mathbf{g} = \frac{1}{c^2} \mathbf{E} \times \mathbf{H}. \quad (11)$$

Our interest is how one might apply the force density (8) to charge-neutral materials and as considered previously [10,26,47,50,51]. For this purpose, we apply (8) in the frequency domain.

In phasor form, Ampere's law in our context becomes

$$\nabla \times \mathbf{H} = i\omega \mathbf{D} = i\omega(\epsilon_0 \mathbf{E} + \mathbf{P}), \quad (12)$$

with complex polarization \mathbf{P} , and Gauss's law for the electric field is

$$\nabla \cdot \epsilon_0 \mathbf{E} = -\nabla \cdot \mathbf{P}. \quad (13)$$

Drawing upon previous interpretations [10,26,50,51], and in reference to (8), one might consider the assignments $\mathbf{J} = i\omega \mathbf{P}$ and $\rho = \rho_P = -\nabla \cdot \mathbf{P}$, with ρ_P the complex polarization charge density.

Because we wish to compute the time average of the force density, which involves the products of quantities with sinusoidal time dependence, we will express the time average of a product between time-harmonic position-dependent scalar quantities $a(\mathbf{r}, t) = \text{Re}[a(\mathbf{r}) \exp(i\omega t)]$ and $b(\mathbf{r}, t) = \text{Re}[b(\mathbf{r}) \exp(i\omega t)]$ as

$$\langle a(\mathbf{r}, t) b(\mathbf{r}, t) \rangle = \frac{1}{2} \text{Re}[a(\mathbf{r}) b^*(\mathbf{r})], \quad (14)$$

where $\langle \cdot \rangle$ is the time-average operator, $\text{Re}[\cdot]$ is the real part operator, and $b^*(\mathbf{r})$ is the complex conjugate of $b(\mathbf{r})$. With this frequency domain interpretation in nonmagnetic materials where $\mathbf{B} = \mu_0(\mathbf{H} + \mathbf{M})$ with $\mathbf{M} = 0$, the time-average force density, assuming sinusoidal steady state conditions in (8) and applying (14) to each term, leads to

$$\langle \mathbf{f}_L \rangle = -\frac{\omega \mu_0}{2} \text{Im}[\mathbf{P} \times \mathbf{H}^*] - \frac{1}{2} \text{Re}[(\nabla \cdot \mathbf{P}) \mathbf{E}^*], \quad (15)$$

where we are using a subscript ‘‘L’’ to denote quantities associated with what we are here calling the ‘‘Lorentz force density.’’ We will apply these terms individually to the field geometry given in Sec. III, with the goal of computing a pressure.

By applying the point form of the electric portion of the Lorentz force ($\mathbf{F}_e = q\mathbf{E}$) to two separated charges in a dipole [52], one can arrive at what is sometimes called the ‘‘Kelvin polarization force’’ [53–58], resulting in the expression $\mathbf{f}_{L,e} = (\mathbf{P} \cdot \nabla) \mathbf{E}$. For clarity, we will specify here that this notation is to be interpreted as $(\mathbf{P} \cdot \nabla) \mathbf{E} = P_x(\partial \mathbf{E} / \partial x) + P_y(\partial \mathbf{E} / \partial y) + P_z(\partial \mathbf{E} / \partial z)$. As opposed to viewing the electric interaction as the electric field exerting force on individual bound charges in the material, this interprets the material as a continuum of electric dipoles, each of which as a unit experiences a force in a spatially varying electric field [47]. Some authors have used this form in place of the $\rho \mathbf{E}$ term in (8) [59], while still referring to the resulting expression as the ‘‘Lorentz force.’’ It will be seen later in Sec. V that the other formulation considered here, that of Einstein and Laub, will differ from (15) in our situation of interest only in that it uses the ‘‘Kelvin polarization force’’ rather than the electric force on polarization charge. As the expressions resulting from the following mathematical

developments will demonstrate, the choice of viewing the electric force as acting on the net charge (as in Lorentz here) or on the material dipoles (as in Einstein-Laub) can affect the predicted distribution of the force density throughout electrically polarized material.

A. Cross term

To find a pressure, we begin by evaluating the z -directed component of the first term of (15) in the bulk of the material by substituting for \mathbf{P} , using $\mathbf{P} = \epsilon_0(\epsilon_r - 1)\mathbf{E}$, as

$$\begin{aligned} \langle f_z \rangle_{\times}^{\text{bulk}}(z) &= \hat{\mathbf{z}} \cdot \left(-\frac{\omega \mu_0}{2} \text{Im}[\mathbf{P} \times \mathbf{H}^*] \right) \\ &= \hat{\mathbf{z}} \cdot -\frac{\omega \mu_0}{2} \epsilon_0 \text{Im}[(\epsilon_r - 1)(\hat{\mathbf{x}} E_x + \hat{\mathbf{z}} E_z) \times (\hat{\mathbf{y}} H_y^*)], \end{aligned} \quad (16)$$

where we are using a subscript ‘‘cross’’ (\times) symbol to denote the cross term's contribution to the force.

After evaluation of the cross and dot products, only one term remains in the argument of the $\text{Im}[\cdot]$ operator,

$$\langle f_z \rangle_{\times}^{\text{bulk}}(z) = -\frac{\omega \mu_0 \epsilon_0}{2} \text{Im}[(\epsilon_r - 1) E_x H_y^*]. \quad (17)$$

We substitute for E_x and H_y^* using (4), giving

$$\begin{aligned} E_x H_y^* &= \left[H_{0i} T_h \frac{k_{tz} \eta}{k} e^{-i(k_x x + k_{tz} z)} \right] \left[H_{0i}^* T_h^* e^{i(k_x x + k_{tz}^* z)} \right] \\ &= |H_{0i}|^2 |T_h|^2 \frac{k_{tz} \eta}{k} e^{2k_{tz}'' z}, \end{aligned} \quad (18)$$

where $k_{tz}'' = \text{Im}[k_{tz}] < 0$. Now, substituting results from (18) into (17) and simplifying, we arrive at

$$\langle f_z \rangle_{\times}^{\text{bulk}}(z) = -\frac{\omega \mu_0 \epsilon_0}{2} |H_{0i}|^2 |T_h|^2 \text{Im} \left[\frac{k_{tz} \eta (\epsilon_r - 1)}{k} \right] e^{2k_{tz}'' z}, \quad (19)$$

indicating an exponential decay of the force density into the bulk of the material. To determine a pressure from a force density as a function of z , we integrate from the material boundary at $z = 0$ to infinity, as

$$P_{\times}^{\text{bulk}} = \int_0^{\infty} \langle f_z \rangle_{\times}^{\text{bulk}}(z) dz. \quad (20)$$

The evaluation of this integral using (19) is given in Appendix C and results in

$$P_{\times}^{\text{bulk}} = \frac{|\langle \mathbf{S}_i \rangle| |T_h|^2}{c} \frac{1}{2} \left(1 - \frac{\sin^2 \theta_i}{|\epsilon_r|^2} + \frac{|\epsilon_r - \sin^2 \theta_i|}{|\epsilon_r|^2} \right). \quad (21)$$

As will be shown below, the nabla term in the Lorentz formulation does not contribute to the bulk force, meaning (21) gives the total force in the bulk of the material, as predicted by the Lorentz formulation.

B. Nabla term in material

For the Lorentz formulation, we will now demonstrate that the second term of (15) is zero within the bulk of the material. This is readily seen since our model accounts for all current in the complex dielectric constant $\epsilon_r = 1 + \chi_E$, and therefore all charge motion is accounted for by the complex polarization density, $\mathbf{P} = \epsilon_0(\epsilon_r - 1)\mathbf{E}$. We can thus write Gauss's Law

using $\mathbf{D} = \epsilon_0 \mathbf{E} + \mathbf{P}$ as

$$\rho = \nabla \cdot (\epsilon_0 \mathbf{E} + \mathbf{P}) = 0. \quad (22)$$

This can be rewritten as

$$\nabla \cdot \mathbf{P} = -\epsilon_0 (\nabla \cdot \mathbf{E}). \quad (23)$$

Substituting for $\mathbf{P} = \epsilon_0 (\epsilon_r - 1) \mathbf{E}$, we have that

$$\epsilon_0 \nabla \cdot [(\epsilon_r(\mathbf{r}) - 1) \mathbf{E}] = -\epsilon_0 (\nabla \cdot \mathbf{E}). \quad (24)$$

Since our field solution obeys Gauss's law, it also obeys (24). In a homogeneous lossy material, we have that the relative electric permittivity ϵ_r is independent of position, and that $\epsilon_r \neq 0$. With these two conditions, the only way (24) can be satisfied is if $\nabla \cdot \mathbf{E} = 0$, meaning that the divergence of the electric field must be zero in the material.¹ It then follows from (23) that $\nabla \cdot \mathbf{P} = 0$ in the material, which shows that the second (nabla) term of (15) is zero in the lossy dielectric (and in free space).

C. Nabla term at boundary

The above line of reasoning does not hold across the surface of the material, however. In our piecewise-constant model for material parameters, $\epsilon_r(\mathbf{r})$ is modeled as a step function in z at $z = 0$, and as such $\nabla \cdot \epsilon_r(\mathbf{r}) \neq 0$ at $z = 0$. This results in both $\nabla \cdot \mathbf{P}$ and \mathbf{E}^* being nonzero from $z = 0^-$ to $z = 0^+$, meaning that the second term of (15) must be evaluated in this infinitesimal region.

We note here that the “surface” and “bulk” contributions described in this paper are referring to those that arise only for p -polarized obliquely incident radiation [26], whose field geometry supports an abrupt change in the normal electric field at the interface. This differs from other analyses of radiation pressure for normal incidence [60], where “surface contribution” is used to describe the momentum transfer that takes place at the boundary between media of different material parameters as the radiation moves from one medium to another and its associated momentum changes accordingly. Here, we use “surface” to refer to pressures due to the abrupt change in normal electric fields and polarization densities at the surface for obliquely incident, p -polarized radiation.

To handle the field discontinuity, we adopt an often-used approach in field theory which uses the arithmetic mean of the field quantities on either side of the discontinuity. This approach was used by Maxwell to compute electrostatic force on a conductive surface with surface charge [61] and has been used by others (see Ref. [26], for example).

To find the total z -directed force due to the second term in (15), we integrate the force density over the infinitesimal surface region at $z = 0$, taking the dot product with $\hat{\mathbf{z}}$ as

$$P_L^{\text{surf.}} = \hat{\mathbf{z}} \cdot \int_{0^-}^{0^+} -\frac{1}{2} \text{Re}[(\nabla \cdot \mathbf{P}) \mathbf{E}^*] dz. \quad (25)$$

The Lorentz interpretation of $-(\nabla \cdot \mathbf{P})$ as a charge density lends itself to the viewing of this surface interaction as the result of the accumulation of surface charge, upon which

the electric field exerts a force. Evaluation of this expression using the field solution in (3) and (4), detailed in Appendix E, results in

$$P_L^{\text{surf.}} = -\frac{|\langle \mathbf{S}_i \rangle| |T_h|^2}{c} \frac{1}{2} \left[\frac{\sin^2 \theta_i}{|\epsilon_r|^2} (|\epsilon_r|^2 - 1) \right]. \quad (26)$$

As will be shown in Sec. VI, the above (26) is precisely the difference between the Maxwell-Bartoli expression (2) and the bulk Lorentz term (21).

D. Total Lorentz pressure

Having evaluated both terms of (15), both in the bulk (21) and across the boundary (26), we can arrive at the total pressure predicted by the Lorentz force density formulation. Adding together the results in (21) and (26), we find that

$$P_L = \frac{|\langle \mathbf{S}_i \rangle| |T_h|^2}{c} \frac{1}{2} \left[1 - \frac{\sin^2 \theta_i}{|\epsilon_r|^2} + \frac{|\epsilon_r - \sin^2 \theta_i|}{|\epsilon_r|^2} - \frac{\sin^2 \theta_i}{|\epsilon_r|^2} (|\epsilon_r|^2 - 1) \right], \quad (27)$$

which simplifies to (using that $1 - \sin^2 \theta_i = \cos^2 \theta_i$)

$$P_L = \frac{|\langle \mathbf{S}_i \rangle| |T_h|^2}{c} \frac{1}{2} \left(\cos^2 \theta_i + \frac{|\epsilon_r - \sin^2 \theta_i|}{|\epsilon_r|^2} \right). \quad (28)$$

V. EINSTEIN-LAUB PRESSURE EVALUATION

We now evaluate the Einstein-Laub force density expression, given in its full form as [9,10]

$$\mathbf{f}_{\text{EL}} = \frac{\partial \mathbf{P}}{\partial t} \times \mu_0 \mathbf{H} - \frac{\partial \mu_0 \mathbf{M}}{\partial t} \times \epsilon_0 \mathbf{E} + \rho \mathbf{E} + \mathbf{J} \times \mu_0 \mathbf{H} + (\mathbf{P} \cdot \nabla) \mathbf{E} + \mu_0 (\mathbf{M} \cdot \nabla) \mathbf{H}. \quad (29)$$

We note that (29) is more explicitly defined in material media than the Lorentz formulation (8). Hence, it does not suffer from the same possible ambiguities in its application to charge-neutral macroscopic media. Note that the first term listed above is (in nonmagnetizable materials) identical to terms we have used in (15), upon time-averaging, and that this formulation explicitly incorporates the so-called “Kelvin polarization force” discussed in Sec. IV as the fifth term in the above (29). The original reason for its inclusion in the force density expression, as stated in Ref. [4], was because it resulted from the calculation of the net electric force on a volume density of infinitesimal electric dipole moments. This is in contrast with the previous approach here called the Lorentz formulation [discussed briefly after (13)], which views the electric field as acting on the net charge density at any point in the material.

The force density (29) obeys a momentum conservation equation analogous to (9), where the Einstein-Laub stress tensor has the form [4,62]

$$\mathbf{T}_{\text{EL}} = \frac{1}{2} (\epsilon_0 \mathbf{E} \cdot \mathbf{E} + \mu_0 \mathbf{H} \cdot \mathbf{H}) \mathbf{I} - \mathbf{DE} - \mathbf{BH}, \quad (30)$$

with associated momentum density [62,63]

$$\mathbf{g}_{\text{EL}} = \frac{1}{c^2} \mathbf{E} \times \mathbf{H}, \quad (31)$$

¹This is also readily verified by direct evaluation of the divergence of the plane wave in (4a).

where this is the same momentum density form as (11), also known as the Abraham momentum [63,64]. Further discussion of this force density formulation and its associated energy-momentum tensor can be found in Sec. 1.2 of Ref. [62].

Upon specification of a single frequency ω in the Fourier domain and time-averaging over one cycle in a nonmagnetic ($\mathbf{M} = 0$), source-free ($\rho, \mathbf{J} = 0$) medium, again using the expression for the time average of the product of two time-harmonic complex quantities given in (14), (29) simplifies to

$$\langle \mathbf{f}_{\text{EL}} \rangle = -\frac{\omega\mu_0}{2} \text{Im}[\mathbf{P} \times \mathbf{H}^*] + \frac{1}{2} \text{Re}[(\mathbf{P} \cdot \nabla)\mathbf{E}^*]. \quad (32)$$

We note that, in applying the full Einstein-Laub formulation (29) to nonmagnetic, source-free media, the only remaining difference between (32) and (15) is that the electric force is applied as the force on a dipole in a spatially varying electric field, rather than the force on bound charges in an electric field. Hence, some might even consider this to be equivalent to an alternative application of the Lorentz force to dielectric media [47]. However, in this work we will refer to (32) as the Einstein-Laub force density and denote quantities associated with it with a subscript ‘‘EL.’’

A. Cross term

We note that the first ‘‘cross’’ term in (32) is exactly the same as the first term of the time-averaged Lorentz expression (15). Therefore for the same field geometry, the first term of the Einstein-Laub expression is also given by (21) for the p -polarized plane wave considered.

B. Nabla term in material

Unlike the Lorentz expression, the second ‘‘nabla’’ term of (32) is nonzero in the bulk of the material. To evaluate for the pressure, we begin by considering the $\hat{\mathbf{z}}$ component of the term,

$$\langle f_{\text{EL},z} \rangle_{\nabla}^{\text{bulk}}(z) = \hat{\mathbf{z}} \cdot \frac{1}{2} \text{Re}[(\mathbf{P} \cdot \nabla)\mathbf{E}^*]. \quad (33)$$

The evaluation and integration of this term is given in Appendix F and results in

$$P_{\text{EL},\nabla}^{\text{bulk}} = -\frac{|\langle \mathbf{S}_i \rangle| |T_h|^2}{c} \left\{ \frac{\sin^2 \theta_i}{|\epsilon_r|^2} [2(\epsilon_r' - 1)] \right\}. \quad (34)$$

C. Nabla term at boundary

Now, to evaluate the nabla term of the Einstein-Laub time-averaged force density given in (32) across the material boundary (from $z = 0^-$ to $z = 0^+$), we proceed in a manner analogous to that in Sec. IV C. The surface term for the Einstein-Laub formulation is

$$P_{\text{EL}}^{\text{surf.}} = \hat{\mathbf{z}} \cdot \int_{0^-}^{0^+} \frac{1}{2} \text{Re}[(\mathbf{P} \cdot \nabla)\mathbf{E}^*] dz. \quad (35)$$

Rather than a viewing the electric field as acting on the net charge, as the Lorentz form did, the $(\mathbf{P} \cdot \nabla)\mathbf{E}$ term in the Einstein-Laub formulation originally stemmed from viewing the spatially varying electric field as acting on a dipole. The

evaluation of this term across the interface is viewed here as the mathematical limiting case of the smooth functions \mathbf{P} and \mathbf{E} being discontinuous across the boundary.

The evaluation of (35) is given in Appendix G and results in

$$P_{\text{EL}}^{\text{surf.}} = -\frac{|\langle \mathbf{S}_i \rangle| |T_h|^2}{c} \left[\frac{\sin^2 \theta_i}{|\epsilon_r|^2} (|\epsilon_r|^2 - 2\epsilon_r' + 1) \right]. \quad (36)$$

Similar to that at the end of Sec. IV C, (36) is also precisely the difference between the Maxwell-Bartoli expression (2) and the Einstein-Laub total bulk contribution [the sum of (21) and (34)], as will be shown in Sec. VI.

D. Total Einstein-Laub pressure

To find the total surface pressure, we sum together the contributions from the cross term of (32) in the bulk [given earlier by (21)], that from the nabla term in the bulk (34), and that from the nabla term across the boundary (36). Upon summation, we find that the expression for the total predicted pressure from the Einstein-Laub formulation is identical to that found for the Lorentz formulation, given in (27) and (28), so $P_{\text{EL}} = P_L = P$ when both bulk and surface contributions are summed.

VI. EQUIVALENCE OF LORENTZ AND EINSTEIN-LAUB PRESSURES TO THE MAXWELL-BARTOLI PRESSURE

We now demonstrate analytically the equivalence of the Lorentz [(28), found from (8)] and Einstein-Laub [shown to be equivalent to the Lorentz form (28) at the end of Sec. V D] pressures to the Maxwell-Bartoli expression (2). First, note that the second term in the square brackets in (28) is equal to $|Z_{zm}|^2/\eta_0^2$, and that we can factor out $\cos^2 \theta_i$ to rewrite (28) as

$$P = \frac{|\langle \mathbf{S}_i \rangle| |T_h|^2}{c} \left(1 + \frac{|Z_{zm}|^2}{\eta_0^2 \cos^2 \theta_i} \right) \cos^2 \theta_i, \quad (37)$$

where the subscript has been removed since this expression was previously shown to result from application of either the Lorentz or Einstein-Laub formulations.

We now also note that $\eta_0^2 \cos^2 \theta_i = |Z_{z0}|^2$, absorb the one in the brackets into the fraction, and by substituting for $|T_h|^2$ using (6), we have

$$P = \frac{|\langle \mathbf{S}_i \rangle|}{c} \left(\frac{2|Z_{z0}|^2}{|Z_{zm} + Z_{z0}|^2} \right) \left(\frac{|Z_{z0}|^2 + |Z_{zm}|^2}{|Z_{z0}|^2} \right) \cos^2 \theta_i. \quad (38)$$

We modify this by making us of the result that for any two complex numbers z_1 and z_2 , it is true that $|z_1|^2 + |z_2|^2 = (|z_1 + z_2|^2 + |z_1 - z_2|^2)/2$. This allows (38) to be written as

$$P = \frac{|\langle \mathbf{S}_i \rangle|}{c} \left(\frac{2}{|Z_{zm} + Z_{z0}|^2} \right) \left(\frac{|Z_{z0} + Z_{zm}|^2 + |Z_{z0} - Z_{zm}|^2}{2} \right) \times \cos^2 \theta_i. \quad (39)$$

After multiplying the two terms in parentheses, it is seen that the first term of the product is 1, and that the second term is $|\Gamma_h|^2$ [see (5)]. Therefore, we have shown analytically that application of either the Lorentz force density formulation (8)

or the Einstein-Laub formulation (29) results in

$$P = \frac{|(\mathbf{S}_i)|}{c} (1 + |\Gamma_h|^2) \cos^2 \theta_i, \quad (40)$$

which is identical to the Maxwell-Bartoli formulation for oblique incidence, given in (2) (now with a differently defined but similar reflection coefficient Γ_h).

VII. APPLICATIONS TO MATERIALS

With analytic expressions for the total, bulk, and surface pressures from the Lorentz and Einstein-Laub formulations, we now apply them to various materials to better understand their behavior. All numerical computations and plots in the following section were generated with MATLAB [65]. All plotted pressure results are normalized, so the expressions developed are normalized (divided) by a factor of $|(\mathbf{S}_i)|/c$.

A. Force density in planar gold

We begin by considering a metal at a visible wavelength as an example of a lossy material. Such plasmonic material is of interest in optomechanics, in part because of the metal-insulator surface waves that exist [66], and in photon drag [67]. Figure 2 shows the angle-dependent results of applying the force density expressions with the material parameters (ϵ_r) of Au at wavelength $\lambda = 650$ nm, where we use $\epsilon_r = -13.28 - i1.128$ [68]. Both the Lorentz and Einstein-Laub formulations provide the same total pressure (the blue curve), as demonstrated above in Sec. VI. However, as shown in Fig. 2, the bulk and surface contributions for the two representations are quite different. The Einstein-Laub formulation (32) predicts a higher magnitude for both the surface and bulk terms than the Lorentz formulation (15). Note also that the surface pressure is negative for all angles other than the endpoints, where it is zero. See Appendix H for discussion on the direction of the surface force. At $\theta_i = 0$, there is no normal component of the electric field, and at $\theta_i = 90^\circ$, the normal component of the incident Poynting vector goes to zero, so there is also zero pressure from the bulk term.

B. Lossless materials

We now turn our attention to the case of lossless materials. Although the developments in Secs. IV–VI required some amount of loss in the bulk pressures to remain valid, we will here consider perturbational loss (the limiting case as $\epsilon_r'' \rightarrow 0$). However, the expressions for outward surface pressure require no amount of loss.

1. Total pressure from both polarizations

We will first consider the angle dependence of the pressure on a lossless dielectric for both s and p polarizations by using (2) and assuming the presence of perturbational loss. In this limit, the bulk contribution to the pressure becomes spread out over infinite depth into the material, but remains finite.

Figure 3 shows the angle dependence of the Maxwell-Bartoli expression (2) for both p and s polarization on a material with refractive index $n = 4$ (and hence $n^2 = \epsilon_r = 16$).

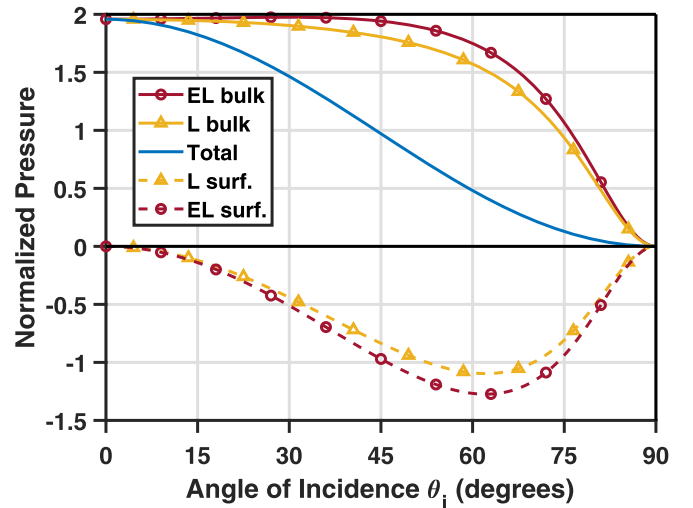


FIG. 2. The bulk, surface, and total force contributions to the radiation pressure due to $\lambda = 650$ nm p -polarized light obliquely incident on planar Au as a function of angle of incidence, normalized (divided) by a factor of $|(\mathbf{S}_i)|/c$. Dashed lines correspond to bulk pressures, dash-dotted lines correspond to surface pressures; circular markers indicate Einstein-Laub (32) predictions, and triangles indicate Lorentz (15) predictions. The solid blue line corresponds to the total pressure, plotted using the Maxwell-Bartoli expression (2). The uppermost red dashed line with circular markers corresponds to the bulk contribution, as predicted by the Einstein-Laub formulation [computed as the sum of (21) and (34)], and the positive yellow dashed line with triangular markers is the bulk pressure predicted by the Lorentz formulation (21). The lower curves are the predicted outward surface pressures (hence the negative values), with the lowermost dash-dotted red curve with circular markers being the Einstein-Laub value (36) and the lower yellow curve with triangular markers being the Lorentz surface pressure (26). Au material parameters for $\lambda = 650$ nm: $\epsilon_r' = -13.28$ and $\epsilon_r'' = -1.128$ [68].

We have not mathematically developed the case of s polarization because the primary interest is in the confined surface pressures that occur mathematically with abrupt changes in the dielectric constant and for the case of p polarization. Since s -polarized radiation has no component of its electric field normal to the material interface, there is no abrupt change in the field giving rise to a surface pressure term [26].

Whereas we defined the magnetic-field reflection coefficient for the case of p polarization (5), we use an analogous definition of the electric-field reflection coefficient for the case of s -polarized radiation (E_y , H_x , H_z , referring to Fig. 1),

$$\Gamma_e = \frac{Z_{zm,e} - Z_{z0,e}}{Z_{zm,e} + Z_{z0,e}} = \frac{E_{yr}}{E_{yi}}, \quad (41)$$

where E_{yi} and E_{yr} are the y -components of the incident and reflected electric fields, respectively, and the z -projected impedances are defined in free space as $Z_{z0,e} = \eta_0 / \cos \theta_i$ and in the material as $Z_{zm,e} = \eta_0 / (\epsilon_r - \sin^2 \theta_i)^{1/2}$. These differ from the z -projected impedances that were used for p polarization, described between (4) and (5). The squared magnitude of this reflection coefficient maintains its interpretation as a power reflection coefficient—in (2), for example.

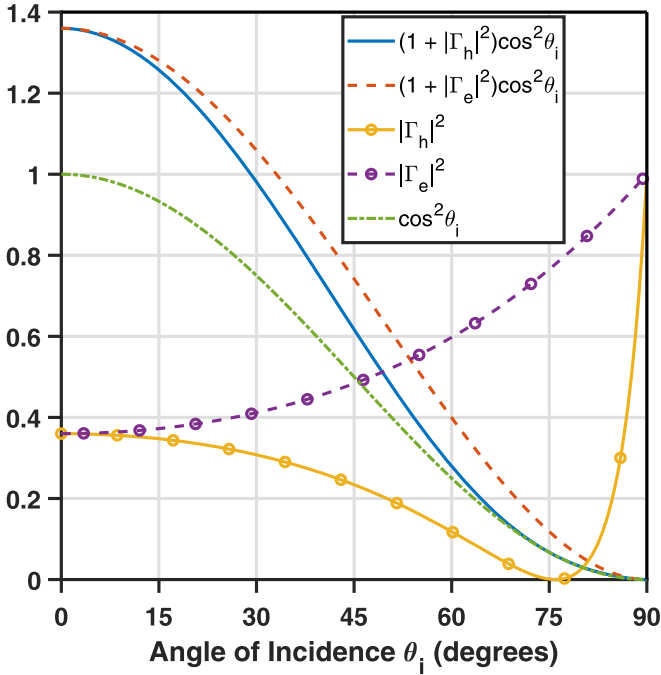


FIG. 3. Curves illustrating the various terms involved in the angle dependence of the Maxwell-Bartoli expression for the case of incidence from free space onto an $n = 4$ material. Solid lines correspond to p polarization and dashed ones to s polarization. The dash-dotted green curve shows the factor of $\cos^2 \theta_i$ alone. The reflection coefficients Γ_h and Γ_e (whose squared magnitudes are plotted here with circular markers) are defined by (5) and (41), with the subscript indicating which field quantity is entirely orthogonal to the plane of incidence. The total expression for p polarization (solid blue) is seen to meet the $\cos^2 \theta_i$ curve at the Brewster angle for $n = 4$, $\theta_B = 75.96^\circ$. It then remains slightly greater than the $\cos^2 \theta_i$ curve for $\theta_B < \theta_i < 90^\circ$.

Figure 3 shows that, for all angles other than normal incidence and 90° , the p -polarization (blue solid line) and s -polarization (red dashed curve) results for pressure determined from (2) are different. The angular dependence of the reflection coefficient magnitude squared is plotted for each polarization. This makes clear the Brewster angle condition for p polarization.

For a lossless dielectric (or in the limiting case of perturbational loss), the condition for the Brewster angle can be written as

$$\sin^2 \theta_B = \frac{\epsilon_r}{\epsilon_r + 1}, \quad (42)$$

where θ_B is used to denote the Brewster angle. For $n = 4$, $\theta_B = 75.96^\circ$, as shown in Fig. 3. At the Brewster angle, the pressure from (2) becomes $P_{MB}|_{\theta_i=\theta_B} = |\langle \mathbf{S}_i \rangle| \cos^2 \theta_B / c$.

2. Surface pressure on water

We now turn our attention to the outward surface pressure alone, whose predicted value requires no assumptions regarding loss. We will consider the case of an air-water interface, because a fluid that could deform in response to a pressure at the interface is a natural choice for the study of such forces. This has been noted, and a number of such experiments have

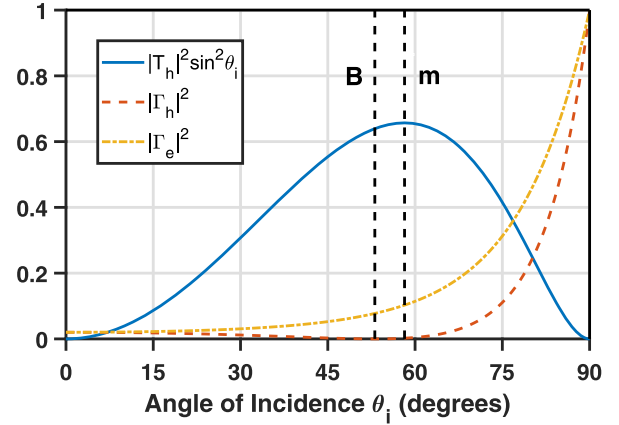


FIG. 4. Curves corresponding to the angle dependence of the predicted outward optical surface pressure and the power reflection coefficients for both p - and s polarizations for a free space-water interface (with $n = 1.331$ at $\lambda = 650$ nm [79]). The solid blue curve shows the angle dependence as in (43), the lower orange dashed curve gives the power reflection coefficient for p polarization $|\Gamma_h|^2$ (5), and the yellow dash-dotted curve gives the power reflection coefficient for s polarization $|\Gamma_e|^2$ (41). Vertical black dashed lines are drawn at the Brewster angle (left, labeled “B”) at $\theta_B = 53.08^\circ$, and at the angle of maximum surface pressure (right, labeled “m”), $\theta_m = 58.19^\circ$.

been performed previously [7,69–75], with various accompanying theoretical analyses [62,76–78].

We first note that both $P_L^{\text{surf.}}$ (26) and $P_{\text{EL}}^{\text{surf.}}$ (36) have the same dependence on angle. That is,

$$P^{\text{surf.}} \propto |T_h|^2 \sin^2 \theta_i \quad (43)$$

for p polarization. It is then simple to find the relationship between the predicted surface pressures using (26) and (36) assuming a lossless material (ϵ_r is purely real and > 1), giving

$$P_L^{\text{surf.}} = \frac{\epsilon_r + 1}{\epsilon_r - 1} P_{\text{EL}}^{\text{surf.}}, \quad (44)$$

where for lossless media the dielectric constant is now simply the square of the real refractive index, $\epsilon_r = n^2$. From here on we speak primarily in terms of refractive indexes rather than dielectric constants as we move to experimental considerations with lossless dielectric materials.

Given its potential experimental value, we consider the case of 650 nm p -polarized light obliquely incident on water. At this wavelength, water has a (real part of the) refractive index of approximately $n = 1.331$ and an extinction coefficient of 1.64×10^{-8} [79]. Since the extinction coefficient is small this case, it is reasonable to treat this material as a lossless dielectric when considering effects near the interface (and having real refractive index n).

Figure 4 shows a plot of the angle dependence given in (43), as well as the power reflection coefficients for both p - and s polarizations using the optical refractive index for water given above. In contrast to the previous dielectric fluid experiments performed at normal incidence [7,69–71,73,75] or oblique incidence with illumination from the side of the fluid [72,74], the phenomenon under investigation here would be the pressure confined to the surface caused by radiation

obliquely incident from the air side of the air-water interface. Moreover, this particular surface pressure is predicted to exist only for p polarization. Hence, a difference in fluid surface deformation between incident radiation polarizations may be observable.

It is also worthy of note for experimental considerations that to observe the deformation of a dielectric fluid such as water, high intensities would likely be required. One way to accomplish this would be to tightly focus a laser beam, whose rapidly varying spatial profile could introduce radial forces that have been claimed to explain the results of the Ashkin and Dziedzic water experiment [10,59,76]. If the beam is focused as such, these potential forces would need to be considered in an experimental setting. Additionally, if observations were to be made using the light reflected (or transmitted) at the interface, the change in reflection and transmission coefficients between polarizations would also need to be considered. These are plotted in Fig. 4.

3. Maximum surface pressure

Given the form of the surface pressure's angle dependence seen in Fig. 4, one may be interested in the angle at which the maximum surface pressure is expected to occur (θ_m) for a lossless dielectric of arbitrary refractive index $n > 1$. This angle at which maximum pressure is predicted to occur of course can be found through direct numerical evaluation of (43) and finding the maximum. Since it is seen in Fig. 4 that there is a single point on the interval $\theta_i \in (0^\circ, 90^\circ)$ at which the angle dependence (43) reaches a local maximum, we can find a condition for this maximum angle by using that the partial derivative of (43) evaluated at θ_m will be equal to zero at the local maximum,

$$\frac{\partial}{\partial \theta_i} (|T_h|^2 \sin^2 \theta_i) \Big|_{\theta_i=\theta_m} = 0. \quad (45)$$

Evaluation of (45) for lossless media (real $\epsilon_r = n^2$) using (6) and the definitions of Z_{z0} and Z_{zm} can be shown to result in the condition

$$\left(\sec \theta_m \sqrt{n^2 - \sin^2 \theta_m} + n^2 \right) \cot \theta_m = \frac{(n^2 - 1) \tan \theta_m \sec \theta_m}{\sqrt{n^2 - \sin^2 \theta_m}}. \quad (46)$$

Equation (46) can be manipulated to eliminate square roots as $n^4[(\tan^2 \theta_m - 1)^2 - (n^2 - \sin^2 \theta_m) \cos^2 \theta_m]$

$$+ [\tan^2 \theta_m \sin^2 \theta_m - 2n^2(\tan^2 \theta_m - 1)] \tan^2 \theta_m \sin^2 \theta_m = 0. \quad (47)$$

The angle θ_m that satisfies (46) and equivalently (47) is the angle of incidence at which the maximum outward surface pressure due to p -polarized radiation is predicted to occur.

Figure 5 shows how θ_m behaves as a function of the refractive index n , as well as the behavior of the predicted maximum surface pressures at $\theta_i = \theta_m$ as a function of n . The angle θ_m is seen to behave differently than the Brewster angle θ_B . In fact, the only place where the two are predicted to coincide, $\theta_m(n) = \theta_B(n)$, is for a material of refractive index $n = 1.554$, where $\theta_m = \theta_B = 57.24^\circ$.

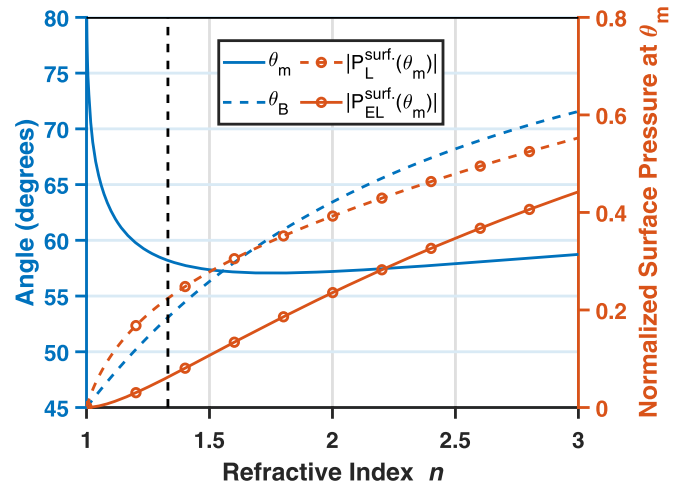


FIG. 5. Behavior of the maximum outward surface pressure on a lossless dielectric as a function of refractive index, $n = \sqrt{\epsilon_r}$. The left blue vertical axis provides the angle scale for the blue curves without markers and the right orange vertical axis provides the normalized outward surface pressure magnitude scale for the orange curves with circular markers. The solid blue curve gives the angle of maximum surface pressure θ_m at each n , computed by numerically solving (47) for θ_m at each value of n . It reaches its lowest value of $\theta_m = 57.06^\circ$ at $n = 1.757$. The dashed blue curve is the Brewster angle θ_B at each n , computed with (42). The dashed and solid orange curves with circular markers are the normalized Lorentz and Einstein-Laub maximum surface pressure magnitudes, computed from (26) and (36), respectively, at incident angle $\theta_i = \theta_m$. We use “normalized” to once again indicate that the specified expressions are divided by a factor of $|\langle S_i \rangle|/c$. A vertical black dashed line is drawn at the refractive index of water used in Sec. VII B 2, $n = 1.331$.

VIII. CONCLUSION

A key issue in determining a force density that allows prediction of experiments relates to the material interface problem treated analytically here and how this folds into the external measure of pressure on condensed matter. In deriving a general relation between the Maxwell-Bartoli pressure and the free space stress tensor with counterpropagating plane waves, we provide a rigorous link between two common ways to describe optical pressure. By showing the equivalence between the angle-dependent Maxwell-Bartoli, Lorentz, and Einstein-Laub pressures, we establish a unified description in terms of the electromagnetic fields external to the material for three widely used models. The Lorentz and Einstein-Laub formulations are shown to predict different distributions of the electromagnetic force between the surface and bulk of the material. The difference between the formulations' predictions can be understood as stemming from their differing respective views of the electric force as acting on the local net charge or on the material dipoles. Future theoretical investigations of more general field and material geometries offer interesting opportunities for insight, such as situations that allow for the excitation of surface plasmons. New experimental studies of angle-dependent optical forces at interfaces will help define a theory. Of note is the opportunity space to experimentally investigate surface pressures with a dielectric fluid for p -polarized obliquely incident radiation.

ACKNOWLEDGMENTS

This work was supported by the Air Force Office of Scientific Research (Grant No. FA9550-19-1-0259), the Army Research Office (Grant No. W911NF-22-2-0245), the National Science Foundation (Grant No. 1927822), and the Defense Advanced Research Projects Agency (Grant No. W911NF-23-1-0043).

APPENDIX A: STRESS TENSOR DERIVATION OF MAXWELL-BARTOLI FOR NORMAL INCIDENCE

Here we present a stress-tensor-based derivation of the Maxwell-Bartoli expression for radiation pressure in the case of normally incident plane-wave radiation. We consider the case of a plane wave reflecting from a material boundary whose position can be considered to remain fixed in space over the timescale of interest. This could be simply due to the inertia of a large object preventing substantial motion over a short period of time, or to some external restoring force that counteracts the radiation pressure (e.g., a mirror mounted physically to a solid surface).

1. Field geometry

To model normally incident radiation reflecting from a material boundary at $z = 0$ back into free space, we write the electric and magnetic fields as superpositions of the forward and backward traveling plane waves using an $\exp(i\omega t)$ time convention as

$$\mathbf{E} = \hat{\mathbf{x}}E_0(e^{-ik_0z} + \Gamma e^{ik_0z}), \quad (\text{A1a})$$

$$\mathbf{H} = \hat{\mathbf{y}}\frac{E_0}{\eta_0}(e^{-ik_0z} - \Gamma e^{ik_0z}), \quad (\text{A1b})$$

where E_0 is the incident peak electric-field amplitude, $\eta_0 = \sqrt{\mu_0/\epsilon_0}$ is the free-space wave impedance, ϵ_0 is vacuum permittivity, μ_0 is vacuum permeability, and Γ is the electric-field reflection coefficient at the material boundary.

To find the pressure on the surface, we introduce the electromagnetic stress tensor formulation for computing electromagnetic forces. This involves the use of a tensor that represents momentum flow through the electromagnetic field, such that a statement of momentum conservation can be written as [10,80]

$$\nabla \cdot \mathbf{T} = -\left(\mathbf{f} + \frac{\partial \mathbf{g}}{\partial t}\right), \quad (\text{A2})$$

where \mathbf{T} is the electromagnetic stress tensor (which may have different formulations), \mathbf{f} is the electromagnetic force density in the material, and \mathbf{g} is the electromagnetic momentum density in the fields.

Without yet specifying a particular form for any quantities involved in terms of fields, we are free to integrate both sides over a volume v bounded by closed surface s and apply Gauss's divergence theorem to the left side of (A2). This results in

$$\oint_s \mathbf{T} \cdot \hat{\mathbf{n}} ds = - \iiint_v \mathbf{f} + \frac{\partial \mathbf{g}}{\partial t} dv, \quad (\text{A3})$$

where $\hat{\mathbf{n}}$ is the outward surface normal unit vector, ds is the differential surface area element of surface s , and dv is the differential volume element of volume v . We are also free to take the time-average of both sides of the equation, resulting in

$$\oint_s \langle \mathbf{T} \rangle \cdot \hat{\mathbf{n}} ds = - \iiint_v \langle \mathbf{f} \rangle + \left\langle \frac{\partial \mathbf{g}}{\partial t} \right\rangle dv. \quad (\text{A4})$$

We now apply the general form in (A4) to the situation of interest with time-harmonic fields. Since all fields of interest are periodic in time (with a period length that will here be denoted by T_p , with a subscript to differentiate it from stress tensor components), it follows that T_p is also a period of any quantities that are functions of the fields, including the electromagnetic momentum density $\mathbf{g}(t)$. Because $\mathbf{g}(t)$ is periodic in time, and T_p is a period [although not necessarily the shortest period of $\mathbf{g}(t)$], it follows that the time-average over T_p of the time derivative of the electromagnetic momentum density is zero ($\langle \partial \mathbf{g} / \partial t \rangle = 0$, see Appendix B for a proof). We note that our material and field geometry are uniform in both x and y . To find a pressure, we construct a closed integration surface in the form of a rectangular prism. One face is parallel to the xy plane of area A , located in free space outside the material at $z = z_0$, with $z_0 < 0$. The four faces perpendicular to the first, with surface normals along $\pm \hat{\mathbf{x}}$ and $\pm \hat{\mathbf{y}}$, extend along the z direction and into the material, out to $z \rightarrow \infty$. The final face of area A is located at $z \rightarrow \infty$, and since our material will be defined as having some amount of loss, the fields (and therefore \mathbf{T}) will have decayed to zero at that face.

Because of the uniformity of the fields in x and y , the pairs of surface faces parallel to the xz and yz planes will have zero contribution to the surface integral of \mathbf{T} . It then follows that the only nonzero contribution to the surface integral is that on the face of area A at $z = z_0 < 0$ with outward surface normal $-\hat{\mathbf{z}}$. Thus, the integral reduces to simple multiplication by the face's area A as

$$\oint_s \langle \mathbf{T} \rangle \cdot \hat{\mathbf{n}} ds = \langle \mathbf{T} \rangle \cdot (-\hat{\mathbf{z}})A = - \iiint_v \langle \mathbf{f} \rangle dv. \quad (\text{A5})$$

The volume integral of the time-average force density is the time-average of the net force on the enclosed volume, \mathbf{F} . Simplifying the dot product on the left-hand side of (A5) as well, we have that

$$(\hat{\mathbf{x}}\langle T_{xz} \rangle + \hat{\mathbf{y}}\langle T_{yz} \rangle + \hat{\mathbf{z}}\langle T_{zz} \rangle)A = \mathbf{F}. \quad (\text{A6})$$

To find the pressure, we now take only the component of the force normal to the surface (the z direction, in this case), and divide it by the area of the surface, A . It follows from the above that

$$\frac{F_z}{A} = P = \langle T_{zz} \rangle. \quad (\text{A7})$$

Equation (A7) indicates that, in this case, the pressure is determined by the time-average of the zz component of the stress tensor.

2. Stress tensor evaluation

We now evaluate the electromagnetic stress tensor using the field expressions given in (A1). The Maxwell stress tensor

in free space is given here by [48,49,64,81,82]

$$\mathbf{T} = \frac{1}{2}(\epsilon_0 \mathbf{E} \cdot \mathbf{E} + \mu_0 \mathbf{H} \cdot \mathbf{H})\mathbf{I} - \epsilon_0 \mathbf{E}\mathbf{E}^* - \mu_0 \mathbf{H}\mathbf{H}^*, \quad (\text{A8})$$

where \mathbf{AB} denotes the dyadic product between two vectors \mathbf{A} and \mathbf{B} , $\mathbf{A} \cdot \mathbf{B}$ is the usual dot product, and \mathbf{I} is the unit dyadic. It is worthy of note that this is also the form that the Einstein-Laub stress tensor assumes in free space ($\mathbf{P} = 0$ and $\mathbf{M} = 0$). Given time-harmonic fields, we can write the time-average of \mathbf{T} as

$$\langle \mathbf{T} \rangle = \frac{1}{2} \text{Re} \left[\frac{1}{2} (\epsilon_0 \mathbf{E} \cdot \mathbf{E}^* + \mu_0 \mathbf{H} \cdot \mathbf{H}^*) \mathbf{I} - \epsilon_0 \mathbf{E}\mathbf{E}^* - \mu_0 \mathbf{H}\mathbf{H}^* \right]. \quad (\text{A9})$$

Using $\mathbf{E} = \hat{\mathbf{x}}E_x$ and $\mathbf{H} = \hat{\mathbf{y}}H_y$ from (A1), we can write (A9) as

$$\langle \mathbf{T} \rangle = \frac{1}{2} \text{Re} \left[\frac{1}{2} (\epsilon_0 E_x E_x^* + \mu_0 H_y H_y^*) (\hat{\mathbf{x}}\hat{\mathbf{x}} + \hat{\mathbf{y}}\hat{\mathbf{y}} + \hat{\mathbf{z}}\hat{\mathbf{z}}) - \hat{\mathbf{x}}\hat{\mathbf{x}}\epsilon_0 E_x E_x^* - \hat{\mathbf{y}}\hat{\mathbf{y}}\mu_0 H_y H_y^* \right]. \quad (\text{A10})$$

With the given electric-field solution in (A1a), we can evaluate the recurring term $\epsilon_0 E_x E_x^*$ as

$$\epsilon_0 E_x E_x^* = \epsilon_0 [E_0 (e^{-ik_0 z} + \Gamma e^{ik_0 z}) E_0^* (e^{ik_0 z} + \Gamma^* e^{-ik_0 z})], \quad (\text{A11})$$

distributing and simplifying to

$$\epsilon_0 E_x E_x^* = \epsilon_0 |E_0|^2 (1 + 2 \text{Re}[\Gamma e^{i2k_0 z}] + |\Gamma|^2). \quad (\text{A12})$$

We can also evaluate the recurring $\mu_0 H_y H_y^*$, which similarly simplifies to

$$\mu_0 H_y H_y^* = \epsilon_0 |E_0|^2 (1 - 2 \text{Re}[\Gamma e^{i2k_0 z}] + |\Gamma|^2). \quad (\text{A13})$$

Using these simplified forms, we can evaluate the term in parentheses in (A10) as

$$\frac{1}{2} (\epsilon_0 E_x E_x^* + \mu_0 H_y H_y^*) = \epsilon_0 |E_0|^2 (1 + |\Gamma|^2), \quad (\text{A14})$$

and upon substituting this back into (A10) with the simplifications from (A12) and (A13), we arrive at

$$\langle \mathbf{T} \rangle = \frac{\epsilon_0 |E_0|^2}{2} [-\hat{\mathbf{x}}\hat{\mathbf{x}}(2 \text{Re}[\Gamma e^{i2k_0 z}]) + \hat{\mathbf{y}}\hat{\mathbf{y}}(2 \text{Re}[\Gamma e^{i2k_0 z}]) + \hat{\mathbf{z}}\hat{\mathbf{z}}(1 + |\Gamma|^2)]. \quad (\text{A15})$$

We can further simplify (A15) by writing $|E_0|^2/2 = |\langle \mathbf{S}_i \rangle| \eta_0$, noting that $\eta_0 \epsilon_0 = 1/c$ to manipulate coefficients, and converting the real part of the complex exponential to a sinusoid, giving

$$\langle \mathbf{T} \rangle = \frac{|\langle \mathbf{S}_i \rangle|}{c} [(\hat{\mathbf{y}}\hat{\mathbf{y}} - \hat{\mathbf{x}}\hat{\mathbf{x}}) 2|\Gamma| \cos(2k_0 z + \phi_\Gamma) + \hat{\mathbf{z}}\hat{\mathbf{z}}(1 + |\Gamma|^2)], \quad (\text{A16})$$

where $|\Gamma|$ and ϕ_Γ are the magnitude and phase, respectively, of the complex-valued $\Gamma = |\Gamma|e^{i\phi_\Gamma}$. We note the presence of $\hat{\mathbf{x}}\hat{\mathbf{x}}$ and $\hat{\mathbf{y}}\hat{\mathbf{y}}$ components of the time-averaged stress tensor that oscillate in z . However, they have no bearing on the pressure on the material, since the pressure depends only on the $\hat{\mathbf{z}}\hat{\mathbf{z}}$ component of the stress tensor. Using the $\hat{\mathbf{z}}\hat{\mathbf{z}}$ component of (A16) in (A7), we find that

$$P = \frac{|\langle \mathbf{S}_i \rangle|}{c} (1 + |\Gamma|^2), \quad (\text{A17})$$

which is the Maxwell-Bartoli expression (2) for normal incidence.

APPENDIX B: TIME AVERAGE OF THE MOMENTUM DENSITY TIME DERIVATIVE

Since $\mathbf{g}(t)$ is periodic in time where T_p is a period, then by definition, for any time t ,

$$\mathbf{g}(t) = \mathbf{g}(t - T_p). \quad (\text{B1})$$

If we define a time average over the period T_p (denoted with $\langle \cdot \rangle$) of any time-varying quantity as

$$\langle f(t) \rangle = \frac{1}{T_p} \int_{t-T_p}^t f(\tau) d\tau, \quad (\text{B2})$$

then the time average of the time derivative of \mathbf{g} is

$$\left\langle \frac{\partial \mathbf{g}}{\partial t} \right\rangle = \frac{1}{T_p} \int_{t-T_p}^t \frac{\partial \mathbf{g}(\tau)}{\partial \tau} d\tau. \quad (\text{B3})$$

By the fundamental theorem of calculus,

$$\frac{1}{T_p} \int_{t-T_p}^t \frac{\partial \mathbf{g}(\tau)}{\partial \tau} d\tau = \frac{1}{T_p} [\mathbf{g}(t) - \mathbf{g}(t - T_p)], \quad (\text{B4})$$

and from the condition of time-periodicity (B1), the quantity in parentheses on the right side of (B4) is zero, resulting in

$$\left\langle \frac{\partial \mathbf{g}}{\partial t} \right\rangle = 0. \quad (\text{B5})$$

Hence, the time average over a period of the time derivative of $\mathbf{g}(t)$ (and generally the time average over a period of the time derivative of any time-periodic quantity) is zero.

APPENDIX C: BULK FORCE DENSITY INTEGRATION

Here we present the evaluation and simplification of the integral in (20) in Sec. IV A. Since the only z dependence in (19) is in the exponential function, this integral is easily evaluated as

$$\int_0^\infty e^{2k''_{tz} z} dz = \frac{e^{2k''_{tz} z}}{2k''_{tz}} \Big|_0^\infty = -\frac{1}{2k''_{tz}} \quad (\text{C1})$$

because the medium is passive and lossy ($k''_{tz} < 0$). Equation (C1) is used with the remainder of (19) to arrive at an expression for the pressure due to the ‘‘cross term’’ of (15) in the bulk of the material, resulting in

$$P_x^{\text{bulk}} = \frac{\omega \mu_0 \epsilon_0}{4k''_{tz}} |H_{0i}|^2 |T_h|^2 \text{Im} \left[\frac{k_{tz} \eta (\epsilon_r - 1)}{k} \right]. \quad (\text{C2})$$

We can then eliminate dependence on ω by making multiple substitutions, first by using

$$k''_{tz} = \text{Im}[k_{tz}] = \text{Im}[\sqrt{k^2 - k_x^2}], \quad (\text{C3})$$

then by substituting $k^2 = k_0^2 \epsilon_r$ and $k_x^2 = k_0^2 \sin^2 \theta_i$, and factoring out k_0 from the square root,

$$k''_{tz} = k_0 \text{Im}[\sqrt{\epsilon_r - \sin^2 \theta_i}], \quad (\text{C4})$$

now assuming that $\theta_i \in [0, \pi/2]$.

We substitute the result in (C4) back into the denominator in (C2), and make use of $k_0 = \omega \sqrt{\mu_0 \epsilon_0}$ to eliminate the ω in

the numerator, resulting in

$$P_{\times}^{\text{bulk}} = \frac{\sqrt{\mu_0 \epsilon_0}}{4 \text{Im}[\sqrt{\epsilon_r - \sin^2 \theta_i}]} |H_{0i}|^2 |T_h|^2 \text{Im} \left[\frac{k_{tz} \eta (\epsilon_r - 1)}{k} \right]. \quad (\text{C5})$$

Now, we can simplify the argument of the rightmost $\text{Im}[\cdot]$ operator in (C5). Once again, we make the substitutions $k_{tz} = (k^2 - k_x^2)^{1/2}$, $k^2 = k_0^2 \epsilon_r$, $k_x^2 = k_0^2 \sin^2 \theta_i$, and $\eta = \eta_0 / \sqrt{\epsilon_r}$ to simplify as

$$\frac{k_{tz} \eta (\epsilon_r - 1)}{k} = \frac{\sqrt{\epsilon_r - \sin^2 \theta_i}}{\epsilon_r} \eta_0 (\epsilon_r - 1). \quad (\text{C6})$$

We substitute this result for the argument of the rightmost $\text{Im}[\cdot]$ operator in (C5), factoring real coefficients outside the operator and using $\eta_0 = \sqrt{\mu_0 / \epsilon_0}$, to arrive at

$$P_{\times}^{\text{bulk}} = \frac{\mu_0}{4} |H_{0i}|^2 |T_h|^2 \frac{\text{Im} \left[\frac{\sqrt{\epsilon_r - \sin^2 \theta_i}}{\epsilon_r} (\epsilon_r - 1) \right]}{\text{Im}[\sqrt{\epsilon_r - \sin^2 \theta_i}]}. \quad (\text{C7})$$

With $|H_{0i}|^2/2 = |\langle \mathbf{S}_i \rangle| / \eta_0$ and $\mu_0 / \eta_0 = 1/c$, we can rewrite some coefficients in a form reminiscent of (2), arriving at

$$P_{\times}^{\text{bulk}} = \frac{|\langle \mathbf{S}_i \rangle| |T_h|^2}{c} \frac{\text{Im} \left[\frac{\sqrt{\epsilon_r - \sin^2 \theta_i}}{\epsilon_r} (\epsilon_r - 1) \right]}{2 \text{Im}[\sqrt{\epsilon_r - \sin^2 \theta_i}]}. \quad (\text{C8})$$

This may be rewritten (strictly assuming that $\epsilon_r'' \neq 0$, although it is valid asymptotically as $\epsilon_r'' \rightarrow 0$) using the result given in Appendix D in (D8) to arrive at the result given in (21),

$$P_{\times}^{\text{bulk}} = \frac{|\langle \mathbf{S}_i \rangle| |T_h|^2}{c} \left[1 - \frac{\sin^2 \theta_i}{|\epsilon_r|^2} + \frac{|\epsilon_r - \sin^2 \theta_i|}{|\epsilon_r|^2} \right]. \quad (\text{C9})$$

APPENDIX D: FRACTION EVALUATION

Here we begin by showing that, for two complex numbers α and β ,

$$\frac{\text{Im}[\alpha\beta]}{\text{Im}[\alpha]} = \frac{\text{Im}[\alpha^2\beta]}{\text{Im}[\alpha^2]} + |\alpha^2| \frac{\text{Im}[\beta]}{\text{Im}[\alpha^2]}, \quad \text{for } \text{Re}[\alpha] \neq 0, \quad (\text{D1})$$

and demonstrate the use of this result in the simplification of (C8).

We start by rewriting the $\text{Im}[\cdot]$ operator using that for any complex number z , $\text{Im}[z] = (z - z^*) / (2i)$, multiplying both numerator and denominator by $\alpha + \alpha^*$ (here requiring that $\text{Re}[\alpha] \neq 0$), and simplifying as

$$\begin{aligned} \frac{\text{Im}[\alpha\beta]}{\text{Im}[\alpha]} &= \frac{\alpha\beta - \alpha^*\beta^*}{\alpha - \alpha^*} \frac{\alpha + \alpha^*}{\alpha + \alpha^*} \\ &= \frac{\alpha^2\beta - (\alpha^2\beta)^* + |\alpha|^2(\beta - \beta^*)}{\alpha^2 - (\alpha^2)^*}. \end{aligned} \quad (\text{D2})$$

Although we require that $\text{Re}[\alpha] \neq 0$ to prevent multiplying by an indeterminate fraction, we note that the expression is asymptotically correct as $\text{Re}[\alpha] \rightarrow 0$.

We now recognize the alternate form of the $\text{Im}[\cdot]$ operation in both numerator and denominator in (D2), such that the

factors of $2i$ cancel, resulting in

$$\frac{\alpha^2\beta - (\alpha^2\beta)^* + |\alpha|^2(\beta - \beta^*)}{\alpha^2 - (\alpha^2)^*} = \frac{\text{Im}[\alpha^2\beta] + |\alpha^2| \text{Im}[\beta]}{\text{Im}[\alpha^2]}, \quad (\text{D3})$$

where we have used that $|\alpha|^2 = |\alpha^2|$ to arrive at the desired result.

We now use the relation given in (D1) to simplify the fraction term in (C8), where we will define $\alpha = (\epsilon_r - \sin^2 \theta_i)^{1/2}$ and $\beta = \chi_E / \epsilon_r = (\epsilon_r - 1) / \epsilon_r$. With these substitutions, we have that some individual terms present in (D1) evaluate as

$$\text{Im}[\alpha^2] = \epsilon_r'', \quad (\text{D4})$$

$$\text{Im}[\beta] = \text{Im} \left[\frac{\epsilon_r - 1}{\epsilon_r} \right] = \text{Im} \left[1 - \frac{\epsilon_r^*}{|\epsilon_r|^2} \right] = \frac{\epsilon_r''}{|\epsilon_r|^2}, \quad (\text{D5})$$

$$\begin{aligned} \alpha^2\beta &= (\epsilon_r - \sin^2 \theta_i) \left(1 - \frac{\epsilon_r^*}{|\epsilon_r|^2} \right) \\ &= \epsilon_r - \sin^2 \theta_i - 1 + \frac{\epsilon_r^* \sin^2 \theta_i}{|\epsilon_r|^2}, \end{aligned} \quad (\text{D6})$$

and hence

$$\text{Im}[\alpha^2\beta] = \epsilon_r'' \left(1 - \frac{\sin^2 \theta_i}{|\epsilon_r|^2} \right). \quad (\text{D7})$$

As for the requirement that $\text{Re}[\alpha] \neq 0$, we note that this can be rewritten equivalently as $\alpha \neq -\alpha^*$. Squaring both sides results in the requirement that $\alpha^2 \neq (\alpha^2)^*$. Substituting the previous definition of α , we find that this is equivalent to $\epsilon_r - \sin^2 \theta_i \neq (\epsilon_r - \sin^2 \theta_i)^*$, or ultimately $\epsilon_r \neq \epsilon_r^*$. This result matches the assumption of some amount of loss, $\epsilon_r'' \neq 0$. We note again here that this expression is still asymptotically correct as $\epsilon_r'' \rightarrow 0$.

Using the simplified forms given above in (D4), (D5), and (D7), and that $\alpha^2 = \epsilon_r - \sin^2 \theta_i$ in the relation (D1), we have shown that the fraction term that appears in (C8) can be simplified as

$$\begin{aligned} &\frac{\text{Im} \left[\frac{\sqrt{\epsilon_r - \sin^2 \theta_i}}{\epsilon_r} (\epsilon_r - 1) \right]}{\text{Im}[\sqrt{\epsilon_r - \sin^2 \theta_i}]} \\ &= 1 - \frac{\sin^2 \theta_i}{|\epsilon_r|^2} + \frac{|\epsilon_r - \sin^2 \theta_i|}{|\epsilon_r|^2}, \quad \text{for } \epsilon_r'' \neq 0. \end{aligned} \quad (\text{D8})$$

APPENDIX E: LORENTZ BOUNDARY EVALUATION

Here we present the evaluation of the integral over the infinitesimal boundary region in (25) in Sec. IV C. Noting from our field solution [(3) and (4)] that the electric field, \mathbf{E} , and therefore the polarization, \mathbf{P} , in this isotropic medium have only $\hat{\mathbf{x}}$ and $\hat{\mathbf{z}}$ components, we can simplify (25) after the dot product as

$$P_L^{\text{surf.}} = -\frac{1}{2} \text{Re} \left[\int_{0^-}^{0^+} \left(\frac{\partial P_x}{\partial x} E_z^* + \frac{\partial P_z}{\partial z} E_x^* \right) dz \right]. \quad (\text{E1})$$

Because both $\partial P_x / \partial x$ and E_z^* remain finite along z , the first term does not contribute. We see, however, that a derivative of the discontinuous field component P_z is present in the integral and hence this will contribute to the integral. Since P_z

is modeled as a step function, from $P_z(0^-) = 0$ to $P_z(0^+) = \epsilon_0(\epsilon_r - 1)E_z(0^+)$, it follows that its derivative in z is in this surface region modeled as a Dirac δ function in z , as

$$\frac{\partial P_z}{\partial z} = P_z(0^+)\delta(z). \quad (\text{E2})$$

Substituting (E2) into (E1), we see that the integral becomes

$$P_L^{\text{surf.}} = -\frac{1}{2} \text{Re} \left[P_z(0^+) \int_{0^-}^{0^+} E_z^* \delta(z) dz \right]. \quad (\text{E3})$$

Since E_z has a discontinuity at $z = 0$, varying from $z = 0^-$ to $z = 0^+$, but remaining finite, we use the arithmetic mean of the field values on either side of the discontinuity when evaluating the integral, which can be thought of as the δ function selecting the midpoint value of E_z^* , resulting in

$$P_L^{\text{surf.}} = -\frac{1}{2} \text{Re} [P_z(0^+) \frac{1}{2} [E_z^*(0^+) + E_z^*(0^-)]]. \quad (\text{E4})$$

We can further simplify by substituting $P_z(0^+) = \epsilon_0(\epsilon_r - 1)E_z(0^+)$ and by using the required continuity of the electric displacement field \mathbf{D} across the boundary, which here manifests as $E_z^*(0^-) = \epsilon_r^* E_z^*(0^+)$. Making both of these substitutions, we have

$$P_L^{\text{surf.}} = -\frac{\epsilon_0}{4} \text{Re} [(\epsilon_r - 1)E_z(0^+) [E_z^*(0^+) + \epsilon_r^* E_z^*(0^+)]]. \quad (\text{E5})$$

After factoring $E_z^*(0^+)$ out of the inner parentheses and distributing the $(\epsilon_r - 1)$, we have

$$P_L^{\text{surf.}} = -\frac{\epsilon_0}{4} \text{Re} [|E_z(0^+)|^2 (|\epsilon_r|^2 - 1 + 2i \text{Im}[\epsilon_r])], \quad (\text{E6})$$

of which we can now trivially take the real part as

$$P_L^{\text{surf.}} = -\frac{\epsilon_0}{4} |E_z(0^+)|^2 (|\epsilon_r|^2 - 1). \quad (\text{E7})$$

We can incorporate a value for $|E_z(0^+)|^2$ by evaluating the squared magnitude of the z component of (4a) at $z = 0$, resulting in

$$P_L^{\text{surf.}} = -\frac{\epsilon_0}{4} |H_{0i}|^2 |T_h|^2 \frac{|\eta|^2}{|k|^2} k_x^2 (|\epsilon_r|^2 - 1). \quad (\text{E8})$$

Substituting $|\eta|^2 = \eta_0^2/|\epsilon_r|$, $|k|^2 = k_0^2|\epsilon_r|$, and $k_x = k_0 \sin \theta_i$, and then using $\eta_0^2 = \mu_0/\epsilon_0$, we can simplify this to

$$P_L^{\text{surf.}} = -\frac{\mu_0}{4} |H_{0i}|^2 |T_h|^2 \left[\frac{\sin^2 \theta_i}{|\epsilon_r|^2} (|\epsilon_r|^2 - 1) \right]. \quad (\text{E9})$$

We can then apply the same simplifications to the coefficients as in (C7) to arrive at the result given in (26),

$$P_L^{\text{surf.}} = -\frac{|\langle \mathbf{S}_i \rangle|}{c} \frac{|T_h|^2}{2} \left[\frac{\sin^2 \theta_i}{|\epsilon_r|^2} (|\epsilon_r|^2 - 1) \right]. \quad (\text{E10})$$

APPENDIX F: EINSTEIN-LAUB NABLA IN MATERIAL EVALUATION

Here we present the evaluation and integration of (33) in Sec. VB. We can simplify the z component of the argument

of the $\text{Re}[\cdot]$ operator in (33) by noting that $P_y = 0$, giving

$$\hat{\mathbf{z}} \cdot (\mathbf{P} \cdot \nabla) \mathbf{E}^* = P_x \frac{\partial E_z^*}{\partial x} + P_z \frac{\partial E_z^*}{\partial z}. \quad (\text{F1})$$

Now we substitute individual components of \mathbf{P} using $\mathbf{P} = \epsilon_0(\epsilon_r - 1)\mathbf{E}$, differentiate with respect to z the complex exponential spatial dependence of E_z^* [as given in (4a)], and factor out $i\epsilon_0(\epsilon_r - 1)$ to arrive at

$$P_x \frac{\partial E_z^*}{\partial x} + P_z \frac{\partial E_z^*}{\partial z} = i\epsilon_0(\epsilon_r - 1)(k_x E_x E_z^* + k_{tz}^* |E_z|^2). \quad (\text{F2})$$

Substituting for E_x and E_z using (4a), we find that

$$\begin{aligned} & i\epsilon_0(\epsilon_r - 1)(k_x E_x E_z^* + k_{tz}^* |E_z|^2) \\ &= i\epsilon_0(\epsilon_r - 1)k_x^2 |H_{0i}|^2 |T_h|^2 \frac{|\eta|^2}{|k|^2} e^{2k_{tz}^* z} (k_{tz}^* - k_{tz}), \end{aligned} \quad (\text{F3})$$

where the difference in the parentheses evaluates as $k_{tz}^* - k_{tz} = -2ik_{tz}''$. Substituting this result back into (F1), we have that

$$\hat{\mathbf{z}} \cdot (\mathbf{P} \cdot \nabla) \mathbf{E}^* = 2\epsilon_0(\epsilon_r - 1)k_{tz}'' k_x^2 |H_{0i}|^2 |T_h|^2 \frac{|\eta|^2}{|k|^2} e^{2k_{tz}'' z}. \quad (\text{F4})$$

Since all terms on the right side of (F4) are real except for ϵ_r , we can easily evaluate the $\text{Re}[\cdot]$ operator as

$$\begin{aligned} \langle f_{\text{EL},z} \rangle_{\nabla}^{\text{bulk}}(z) &= \hat{\mathbf{z}} \cdot \frac{1}{2} \text{Re}[(\mathbf{P} \cdot \nabla) \mathbf{E}^*] \\ &= \epsilon_0(\epsilon_r' - 1)k_{tz}'' k_x^2 |H_{0i}|^2 |T_h|^2 \frac{|\eta|^2}{|k|^2} e^{2k_{tz}'' z}. \end{aligned} \quad (\text{F5})$$

To find the pressure due to the force density, we now integrate (F5) from $z = 0^+$ (avoiding the boundary, which will be handled separately) to $z \rightarrow \infty$. Since this bulk force density has the same spatial dependence as the Lorentz form in Sec. IV A, the integration results in the same factor of $-1/(2k_{tz}'')$, as in (C1). Therefore, after integrating (F5), the pressure due to the nabla term of (32) is given by

$$P_{\text{EL},\nabla}^{\text{bulk}} = -\frac{1}{2} |H_{0i}|^2 |T_h|^2 \epsilon_0 k_x^2 \frac{|\eta|^2}{|k|^2} (\epsilon_r' - 1). \quad (\text{F6})$$

With substitutions analogous to those made between (E8) and (E9), (F6) becomes

$$P_{\text{EL},\nabla}^{\text{bulk}} = -\frac{\mu_0}{4} |H_{0i}|^2 |T_h|^2 \left\{ \frac{\sin \theta_i}{|\epsilon_r|^2} [2(\epsilon_r' - 1)] \right\}, \quad (\text{F7})$$

and we can again manipulate the coefficients as was done between (C7) and (C8) to arrive at the result given in (34),

$$P_{\text{EL},\nabla}^{\text{bulk}} = -\frac{|\langle \mathbf{S}_i \rangle|}{c} \frac{|T_h|^2}{2} \left\{ \frac{\sin^2 \theta_i}{|\epsilon_r|^2} [2(\epsilon_r' - 1)] \right\}. \quad (\text{F8})$$

APPENDIX G: EINSTEIN-LAUB NABLA AT BOUNDARY EVALUATION

Here we present the evaluation of the integration over the infinitesimal boundary region in (35) in Sec. VC. For the field geometry of interest, (35) simplifies to

$$P_{\text{EL}}^{\text{surf.}} = \frac{1}{2} \text{Re} \left[\int_{0^-}^{0^+} \left(P_x \frac{\partial E_z^*}{\partial x} + P_z \frac{\partial E_z^*}{\partial z} \right) dz \right]. \quad (\text{G1})$$

Because $P_x(\partial E_z^*/\partial x)$ remains finite over the interval $z = 0^-$ to $z = 0^+$, it does not contribute to the integral. Now, since E_z is considered as a step function in our model, its derivative will be represented as a Dirac δ function in the surface region, so

$$\frac{\partial E_z^*}{\partial z} = [E_z^*(0^+) - E_z^*(0^-)]\delta(z). \quad (\text{G2})$$

The integral in (G1) then becomes

$$P_{\text{EL}}^{\text{surf.}} = \frac{1}{2} \text{Re} \left[[E_z^*(0^+) - E_z^*(0^-)] \int_{0^-}^{0^+} P_z \delta(z) dz \right]. \quad (\text{G3})$$

As in (E3), we will evaluate the integral using the arithmetic mean of the values of P_z on either side of the boundary. Noting that $P_z(0^-) = 0$, we have

$$P_{\text{EL}}^{\text{surf.}} = \frac{1}{2} \text{Re} \left[[E_z^*(0^+) - E_z^*(0^-)] \frac{1}{2} P_z(0^+) \right]. \quad (\text{G4})$$

Now we can again simplify, as was done for (E4), by substituting $P_z(0^+) = \epsilon_0(\epsilon_r - 1)E_z(0^+)$, and making use of the boundary condition $E_z^*(0^-) = \epsilon_r^* E_z^*(0^+)$, yielding

$$P_{\text{EL}}^{\text{surf.}} = \frac{1}{4} \text{Re} \left[[E_z^*(0^+) - \epsilon_r^* E_z^*(0^+)] [\epsilon_0(\epsilon_r - 1)E_z(0^+)] \right], \quad (\text{G5})$$

which reduces to

$$P_{\text{EL}}^{\text{surf.}} = -\frac{\epsilon_0}{4} |E_z(0^+)|^2 (|\epsilon_r|^2 - 2\epsilon_r' + 1). \quad (\text{G6})$$

We can substitute for $|E_z(0^+)|^2$ by evaluating the squared magnitude of (4a) at $z = 0^+$, once again making substitutions analogous to those made between (E8) and (E9), and manipulating the coefficients to arrive at the result given in (36),

$$P_{\text{EL}}^{\text{surf.}} = -\frac{|\langle \mathbf{S}_i \rangle| |T_h|^2}{c} \frac{1}{2} \left[\frac{\sin^2 \theta_i}{|\epsilon_r|^2} (|\epsilon_r|^2 - 2\epsilon_r' + 1) \right]. \quad (\text{G7})$$

APPENDIX H: CONDITIONS FOR OUTWARD SURFACE FORCES

In Sec. VII, it was shown that for the cases of planar Au and water, the surface force was always directed outward from the material. Here we will show under what conditions the two force formulations, Lorentz and Einstein-Laub, predict a surface force directed away from the medium of interest. The case of complex time-harmonic fields will be considered here, although the development is also easily adapted to static fields by making all quantities real and omitting the time averaging $\{(1/2) \text{Re}[\cdot]\}$ operation.

We consider the situation of a planar interface between two linear isotropic materials, where the interface lies in the xy plane. We denote all $z < 0$ as Region 1 and all $z > 0$ as Region 2. These two regions will have complex relative permittivities of $\epsilon_{r,1}$ and $\epsilon_{r,2}$, respectively. For example, in the situation described in Sec. III and depicted in Fig. 1, $\epsilon_{r,1} = 1$ and $\epsilon_{r,2} = \epsilon_r$. We denote the values of the z component of the electric field (which is perpendicular to the interface) in Regions 1 and 2 by $E_{z,1}$ and $E_{z,2}$, respectively. The values of the z component of the polarization density in Regions 1 and 2 will be similarly denoted by $P_{z,1}$ and $P_{z,2}$, respectively. We consider the source term of Gauss's law to be zero in this situation, such that the perpendicular \mathbf{D} is required to be

continuous. This results in the boundary condition

$$E_{z,2} = \left(\frac{\epsilon_{r,1}}{\epsilon_{r,2}} \right) E_{z,1}. \quad (\text{H1})$$

Additionally, because the media are linear and isotropic, the polarization is related to the electric field in either region by

$$P_{z,n} = \epsilon_0(\epsilon_{r,n} - 1)E_{z,n} = \epsilon_0 \chi_{E,n} E_{z,n}, \quad (\text{H2})$$

where $n = 1, 2$ denotes the region number.

With Region 2 defined as being the space where $z > 0$, our goal of finding when the time-average surface pressure is directed away from Region 2 now is equivalent to finding when the time-average surface pressure is less than zero.

1. Lorentz

Using the approach taken in Sec. IV C, the time-average Lorentz z -directed surface force in this situation is given by

$$\langle P_{\text{L}}^{\text{surf.}} \rangle = \frac{1}{2} \text{Re} \left[\frac{1}{2} (E_{z,1} + E_{z,2})(P_{z,1}^* - P_{z,2}^*) \right]. \quad (\text{H3})$$

Using (H1) and (H2) to rewrite all quantities in (H3) in terms of $E_{z,1}$ and the material parameters results in

$$\langle P_{\text{L}}^{\text{surf.}} \rangle = \frac{1}{4} \text{Re} \left[\epsilon_0 |E_{z,1}|^2 \left(\frac{\epsilon_{r,1}}{\epsilon_{r,2}} + 1 \right) \left[\left(\frac{\epsilon_{r,1}}{\epsilon_{r,2}} \right)^* - 1 \right] \right]. \quad (\text{H4})$$

Further manipulation leads to

$$\langle P_{\text{L}}^{\text{surf.}} \rangle = \frac{\epsilon_0 |E_{z,1}|^2}{4} \text{Re} \left[\left| \frac{\epsilon_{r,1}}{\epsilon_{r,2}} \right|^2 - 1 - 2i \text{Im} \left[\frac{\epsilon_{r,1}}{\epsilon_{r,2}} \right] \right], \quad (\text{H5})$$

of which the real part can be taken to arrive at

$$\langle P_{\text{L}}^{\text{surf.}} \rangle = \frac{\epsilon_0 |E_{z,1}|^2}{4} \left(\left| \frac{\epsilon_{r,1}}{\epsilon_{r,2}} \right|^2 - 1 \right). \quad (\text{H6})$$

It follows from the term in parentheses in (H6) that $\langle P_{\text{L}}^{\text{surf.}} \rangle < 0$ if

$$|\epsilon_{r,2}| > |\epsilon_{r,1}|. \quad (\text{H7})$$

Using the boundary condition (H1) in the inequality (H7) also results in a condition in terms of the electric fields in each region,

$$|E_{z,1}| > |E_{z,2}|. \quad (\text{H8})$$

The Lorentz time-average surface force will be directed away from Region 2 if the equivalent conditions (H7) and (H8) are met.

2. Einstein-Laub

Paralleling the approach in Sec. V C, the time-average Einstein-Laub surface force is given by

$$\langle P_{\text{EL}}^{\text{surf.}} \rangle = \frac{1}{2} \text{Re} \left[\frac{1}{2} (P_{z,1} + P_{z,2})(E_{z,2}^* - E_{z,1}^*) \right]. \quad (\text{H9})$$

Use of (H1) and (H2) allows for the rewriting of (H9) as

$$\langle P_{\text{EL}}^{\text{surf.}} \rangle = \frac{\epsilon_0 |E_{z,1}|^2}{4} \text{Re} \left[1 - \left| \frac{\epsilon_{r,1}}{\epsilon_{r,2}} \right|^2 + 2\epsilon_{r,2} \left| \frac{\epsilon_{r,1}}{\epsilon_{r,2}} \right|^2 - 2\epsilon_{r,1} + 2i \text{Im} \left[\frac{\epsilon_{r,1}}{\epsilon_{r,2}} \right] \right], \quad (\text{H10})$$

where evaluation of the $\text{Re}[\cdot]$ operator results in

$$\langle P_{\text{EL}}^{\text{surf.}} \rangle = \frac{\epsilon_0 |E_{z,1}|^2}{4} \left[1 - 2\epsilon'_{r,1} - \left| \frac{\epsilon_{r,1}}{\epsilon_{r,2}} \right|^2 (1 - 2\epsilon'_{r,2}) \right], \quad (\text{H11})$$

with $\epsilon'_{r,n} = \text{Re}[\epsilon_{r,n}]$. It follows from the contents of the square brackets in (H11) that the condition for negative time-average surface pressure ($\langle P_{\text{EL}}^{\text{surf.}} \rangle < 0$) is

$$\frac{1 - 2\epsilon'_{r,2}}{|\epsilon_{r,2}|^2} > \frac{1 - 2\epsilon'_{r,1}}{|\epsilon_{r,1}|^2}. \quad (\text{H12})$$

Using that $|\chi_E|^2 = |\epsilon_r - 1|^2 = |\epsilon_r|^2 - 2\epsilon'_r + 1$, the numerators in (H12) can be rewritten as

$$\frac{|\chi_{E,2}|^2 - |\epsilon_{r,2}|^2}{|\epsilon_{r,2}|^2} > \frac{|\chi_{E,1}|^2 - |\epsilon_{r,1}|^2}{|\epsilon_{r,1}|^2}, \quad (\text{H13})$$

which can be simplified to the condition

$$\frac{|\chi_{E,2}|}{|\epsilon_{r,2}|} > \frac{|\chi_{E,1}|}{|\epsilon_{r,1}|}. \quad (\text{H14})$$

If (H14) is satisfied by the material parameters, the Einstein-Laub time-average surface force will be directed away from Region 2. Once again, we can seek a condition in terms of field quantities for more physical insight. Making use of (H1), (H14) is equivalently

$$|E_{z,2}| |\chi_{E,2}| > |E_{z,1}| |\chi_{E,1}|. \quad (\text{H15})$$

Finally, because $|P_z| = \epsilon_0 |\chi_E| |E_z|$, the condition for $\langle P_{\text{EL}}^{\text{surf.}} \rangle < 0$ in terms of field quantities is

$$|P_{z,2}| > |P_{z,1}|. \quad (\text{H16})$$

-
- [1] J. C. Maxwell, *A Treatise on Electricity and Magnetism*, 3rd ed. (Dover, New York, 1954) This is an unabridged, unaltered, republication of the third edition, published by the Clarendon Press, Oxford, in 1891. All other references to this title refer to this republication.
- [2] A. G. Bartoli, *Sopra i Movimenti Prodotti dalla Luce e dal Calore: E Sopra il Radiometro di Crookes* (Coi tipi dei successori Le Monnier, 1876) The relevant portion (pp. 22–27) was reprinted verbatim in *Nuovo Cimento* in 1884.
- [3] A. Bartoli, Il calorico raggianti e il secondo principio di termodinamica, *Nuovo Cimento* **15**, 193 (1884). The expression for pressure is given as (1) on p. 197. E is “the mechanical equivalent of heat.” In modern terminology, a unit conversion factor between thermal energy in calories to mechanical energy in joules.
- [4] A. Einstein and J. Laub, Über die im elektromagnetischen Felde auf ruhende Körper ausgeübten ponderomotorischen Kräfte, *Ann. Phys. (Leipzig, Ger.)* **331**, 541 (1908), an English translation is available in Ref. [82].
- [5] E. F. Nichols and G. F. Hull, A preliminary communication on the pressure of heat and light radiation, *Phys. Rev.* **13**, 307 (1901).
- [6] P. N. Lebedew, Untersuchungen über die Druckkräfte des Lichtes, *Ann. Phys. (Leipzig, Ger.)* **311**, 433 (1901) The Maxwell-Bartoli expression is given on p. 434.
- [7] A. Ashkin and J. M. Dziedzic, Radiation Pressure on a Free Liquid Surface, *Phys. Rev. Lett.* **30**, 139 (1973).
- [8] R. V. Jones and B. Leslie, The measurement of optical radiation pressure in dispersive media, *Proc. R. Soc. London, Ser. A* **360**, 347 (1978).
- [9] K. J. Webb, Relationship between the Einstein-Laub electromagnetic force and the Lorentz force on free charge, *Phys. Rev. B* **94**, 064203 (2016).
- [10] M. Mansuripur, A. R. Zakharian, and E. M. Wright, Electromagnetic-force distribution inside matter, *Phys. Rev. A* **88**, 023826 (2013).
- [11] R. N. C. Pfeifer, T. A. Nieminen, N. R. Heckenberg, and H. Rubinsztein-Dunlop, Colloquium: Momentum of an electromagnetic wave in dielectric media, *Rev. Mod. Phys.* **79**, 1197 (2007).
- [12] G. K. Campbell, A. E. Leanhardt, J. Mun, M. Boyd, E. W. Streed, W. Ketterle, and D. E. Pritchard, Photon Recoil Momentum in Dispersive Media, *Phys. Rev. Lett.* **94**, 170403 (2005).
- [13] S. M. Barnett, Resolution of the Abraham-Minkowski Dilemma, *Phys. Rev. Lett.* **104**, 070401 (2010).
- [14] B. A. Kemp, Resolution of the Abraham-Minkowski debate: Implications for the electromagnetic wave theory of light in matter, *J. Appl. Phys.* **109**, 111101 (2011).
- [15] M. G. Silveirinha, Reexamination of the Abraham-Minkowski dilemma, *Phys. Rev. A* **96**, 033831 (2017).
- [16] I. Brevik, Analysis of recent interpretations of the Abraham-Minkowski problem, *Phys. Rev. A* **98**, 043847 (2018).
- [17] S. F. Tolić-Nørrelykke, E. Schäffer, J. Howard, F. S. Pavone, F. Jülicher, and H. Flyvbjerg, Calibration of optical tweezers with positional detection in the back focal plane, *Rev. Sci. Instrum.* **77**, 103101 (2006).
- [18] A. Ashkin, J. M. Dziedzic, J. E. Bjorkholm, and S. Chu, Observation of a single-beam gradient force optical trap for dielectric particles, *Opt. Lett.* **11**, 288 (1986).
- [19] J. R. Moffitt, Y. R. Chemla, S. B. Smith, and C. Bustamante, Recent advances in optical tweezers, *Annu. Rev. Biochem.* **77**, 205 (2008).
- [20] S. Chu, J. E. Bjorkholm, A. Ashkin, and A. Cable, Experimental Observation of Optically Trapped Atoms, *Phys. Rev. Lett.* **57**, 314 (1986).
- [21] I. Liberal, I. Ederra, R. Gonzalo, and R. W. Ziolkowski, Electromagnetic force density in electrically and magnetically polarizable media, *Phys. Rev. A* **88**, 053808 (2013).
- [22] L. Cui, N. Wang, and J. Ng, Computation of internal optical forces using the Helmholtz tensor, *Phys. Rev. A* **104**, 013508 (2021).
- [23] R. Alaee, J. Christensen, and M. Kadic, Optical pulling and pushing forces in bilayer \mathcal{PT} -symmetric structures, *Phys. Rev. Appl.* **9**, 014007 (2018).
- [24] N. A. Mortensen, Mesoscopic electrodynamics at metal surfaces: From quantum-corrected hydrodynamics to microscopic surface-response formalism, *Nanophotonics* **10**, 2563 (2021).
- [25] Z. F. Öztürk, S. Xiao, M. Yan, M. Wubs, A.-P. Jauho, and N. A. Mortensen, Field enhancement at metallic interfaces due to quantum confinement, *J. Nanophotonics* **5**, 051602 (2011).
- [26] M. Mansuripur, Radiation pressure and the linear momentum of the electromagnetic field, *Opt. Express* **12**, 5375 (2004).

- [27] M. Mansuripur, On the foundational equations of the classical theory of electrodynamics, *Resonance* **18**, 130 (2013).
- [28] J. C. Maxwell, *A Treatise on Electricity and Magnetism*, 3rd ed. (Dover, New York, 1954), Vol. 2, Chap. 20.
- [29] J. C. Maxwell, *A Treatise on Electricity and Magnetism*, 3rd ed. (Dover, New York, 1954), Vol. 2, Chap. 20, p. 441.
- [30] B. Carazza and H. Kragh, Adolfo Bartoli and the problem of radiant heat, *Ann. Sci.* **46**, 183 (1989).
- [31] E. F. Nichols and G. F. Hull, The pressure due to radiation (second paper), *Phys. Rev.* **17**, 26 (1903). The Maxwell-Bartoli expression is given on p. 31.
- [32] D. S. Bradshaw and D. L. Andrews, Manipulating particles with light: Radiation and gradient forces, *Eur. J. Phys.* **38**, 034008 (2017), see Eq. (17) for the Maxwell-Bartoli pressure in a slightly different notation.
- [33] M. K. E. L. Planck, *The Theory of Heat Radiation* (Dover Publications, New York, 1991), translated by M. Mausius from the 1914 German edition.
- [34] J. D. Jackson, *Classical Electrodynamics*, 3rd ed. (John Wiley & Sons, Inc., New York, 1999), Chap. I.1, p. 3.
- [35] O. Darrigol, *Electrodynamics from Ampère to Einstein* (Oxford University Press, New York, 2000), p. 327.
- [36] H. A. Lorentz, *Versuch einer Theorie der electrischen und optischen Erscheinungen in bewegten Körpern* (E. J. Brill, Leiden, Netherlands, 1895), this was reprinted in Refs. [37] and [38].
- [37] H. A. Lorentz, *Versuch einer Theorie der electrischen und optischen Erscheinungen in bewegten Körpern* (B. G. Teubner, Leipzig, Ger., 1906).
- [38] H. A. Lorentz, Versuch einer theorie der electrischen und optischen Erscheinungen in bewegten Körpern, in *H. A. Lorentz Collected Papers* (Springer, Dordrecht, Netherlands, 1937), Vol. 5, pp. 1–138.
- [39] J. A. Stratton, *Electromagnetic Theory* (John Wiley & Sons, Hoboken, 2007), Chap. 2.5, pp. 96 and 97.
- [40] H. A. Lorentz, La théorie électromagnétique de Maxwell et son application aux corps mouvants, *Arch. Néerland. des Sciences exactes et naturelles* **25**, 363 (1892), see Eq. (61) on p. 443 for the force on a charge continuum. This paper was reprinted in Ref. [41].
- [41] H. A. Lorentz, La théorie électromagnétique de Maxwell et son application aux corps mouvants, in *H. A. Lorentz Collected Papers* (Springer, Dordrecht, Netherlands, 1936), Vol. 2, pp. 164–321, see Eq. (61) on p. 238 for force formulation.
- [42] P. J. Nahin, *Oliver Heaviside: Sage in Solitude* (IEEE Press, New York, 1988), pp. 119 and 120.
- [43] J. J. Thompson, On the electric and magnetic effects produced by the motion of electrified bodies, *Philos. Mag.* **11**, 229 (1881).
- [44] O. Heaviside, On the electromagnetic effects due to the motion of electrification through a dielectric, *Philos. Mag.* **27**, 324 (1889). See Eq. (4) on p. 326. This was reprinted in Ref. [45].
- [45] O. Heaviside, On the electromagnetic effects due to the motion of electrification through a dielectric, in *Electrical Papers* (Macmillan & Co., New York, NY, 1892), Vol. 2, p. 506.
- [46] J. C. Maxwell, On physical lines of force (part II) (continued): The theory of molecular vortices applied to electric currents, *Philos. Mag.* **21**, 338 (1861), see Eq. (77) on p. 342 for an expression for electromotive force that includes both electric and motional magnetic contributions.
- [47] S. M. Barnett and R. Loudon, On the electromagnetic force on a dielectric medium, *J. Phys. B: At., Mol. Opt. Phys.* **39**, S671 (2006).
- [48] J. D. Jackson, *Classical Electrodynamics*, 3rd ed. (John Wiley & Sons, Inc., New York, 1999), Chap. 6.7, pp. 258–262.
- [49] D. J. Griffiths, *Introduction to Electrodynamics*, 4th ed. (Pearson Education, Boston, MA, 2013), Chap. 8.2.2, pp. 362–364.
- [50] A. R. Zakharian, M. Mansuripur, and J. V. Moloney, Radiation pressure and the distribution of electromagnetic force in dielectric media, *Opt. Express* **13**, 2321 (2005).
- [51] B. A. Kemp, T. M. Grzegorzczuk, and J. A. Kong, Ab initio study of the radiation pressure on dielectric and magnetic media, *Opt. Express* **13**, 9280 (2005).
- [52] H. A. Haus and J. R. Melcher, *Electromagnetic Fields and Energy* (Prentice Hall, Englewood Cliffs, 1989), Chap. 11.8, p. 505.
- [53] H. A. Haus and J. R. Melcher, *Electromagnetic Fields and Energy* (Prentice Hall, Englewood Cliffs, 1989), Chap. 11.9, pp. 514–515.
- [54] S. Schmid, C. Hierold, and A. Boisen, Modeling the Kelvin polarization force actuation of micro- and nanomechanical systems, *J. Appl. Phys.* **107**, 054510 (2010).
- [55] V. I. Pavlov, On discussions concerning the problem of ponderomotive forces, *Sov. Phys. Usp.* **21**, 171 (1978), see their Ref. [13] near Eq. (1), where p. 32 of Ref. [58] is pointed out in particular.
- [56] W. Thomson, On the mathematical theory of electricity in equilibrium, *Camb. Dublin Math. J.* **1** (1845), reprinted in Refs. [57] and [58].
- [57] W. Thomson, On the mathematical theory of electricity in equilibrium, *Philos. Mag.* **8**, 42 (1854), see p. 55.
- [58] W. Thomson, *Reprint of Papers on Electrostatics and Magnetism* (Macmillan & Co., London, 1872), pp. 15–37, see p. 32.
- [59] R. Loudon, Theory of the forces exerted by Laguerre-Gaussian light beams on dielectrics, *Phys. Rev. A* **68**, 013806 (2003). See Eq. (5.1).
- [60] R. Loudon, Theory of the radiation pressure on dielectric surfaces, *J. Mod. Opt.* **49**, 821 (2002).
- [61] J. C. Maxwell, *A Treatise on Electricity and Magnetism*, 3rd ed. (Dover, New York, 1954), Vol. 1, Chap. 1, pp. 161–162.
- [62] I. Brevik, Experiments in phenomenological electrodynamics and the electromagnetic energy-momentum tensor, *Phys. Rep.* **52**, 133 (1979).
- [63] K. J. Webb, Dependence of the Radiation Pressure on the Background Refractive Index, *Phys. Rev. Lett.* **111**, 043602 (2013).
- [64] P. Penfield and H. A. Haus, *Electrodynamics of Moving Media*, M.I.T. Research Monograph Series No. 40 (MIT Press, Cambridge, 1967).
- [65] *MATLAB version 9.5.0.944444 (R2018b)* (The Mathworks, Inc., Natick, Massachusetts, 2018).
- [66] L.-F. Yang, A. Datta, Y.-C. Hsueh, X. Xu, and K. J. Webb, Demonstration of Enhanced Optical Pressure on a Structured Surface, *Phys. Rev. Lett.* **122**, 083901 (2019).
- [67] J. H. Strait, G. Holland, W. Zhu, C. Zhang, B. R. Ilic, A. Agrawal, D. Pacifici, and H. J. Lezec, Revisiting the Photon-Drag Effect in Metal Films, *Phys. Rev. Lett.* **123**, 053903 (2019).

- [68] R. L. Olmon, B. Slovick, T. W. Johnson, D. Shelton, S.-H. Oh, G. D. Boreman, and M. B. Raschke, Optical dielectric function of gold, *Phys. Rev. B* **86**, 235147 (2012).
- [69] K. Sakai, D. Mizuno, and K. Takagi, Measurement of liquid surface properties by laser-induced surface deformation spectroscopy, *Phys. Rev. E* **63**, 046302 (2001).
- [70] A. Casner and J.-P. Delville, Giant Deformations of a Liquid-Liquid Interface Induced by the Optical Radiation Pressure, *Phys. Rev. Lett.* **87**, 054503 (2001).
- [71] A. Casner and J.-P. Delville, Laser-Induced Hydrodynamic Instability of Fluid Interfaces, *Phys. Rev. Lett.* **90**, 144503 (2003).
- [72] O. Emile and J. Emile, Low-Power Laser Deformation of an Air-Liquid Interface, *Phys. Rev. Lett.* **106**, 183904 (2011).
- [73] N. G. C. Astrath, L. C. Malacarne, M. L. Baesso, G. V. B. Lukasiewicz, and S. E. Bialkowski, Unravelling the effects of radiation forces in water, *Nat. Commun.* **5**, 4363 (2014).
- [74] G. Verma and K. P. Singh, Universal Long-Range Nanometric Bending of Water by Light, *Phys. Rev. Lett.* **115**, 143902 (2015).
- [75] N. G. C. Astrath, G. A. Flizikowski, B. Anghinoni, L. C. Malacarne, M. L. Baesso, T. Požar, M. Partanen, I. Brevik, D. Razansky, and S. E. Bialkowski, Unveiling bulk and surface radiation forces in a dielectric liquid, *Light: Sci. Appl.* **11**, 103 (2022).
- [76] R. Loudon, Radiation pressure and momentum in dielectrics, *Fortschr. Phys.* **52**, 1134 (2004).
- [77] A. Hallanger, I. Brevik, S. Haaland, and R. Sollie, Non-linear deformations of liquid-liquid interfaces induced by electromagnetic radiation pressure, *Phys. Rev. E* **71**, 056601 (2005).
- [78] M. Partanen, B. Anghinoni, N. G. C. Astrath, and J. Tulkki, Time-dependent theory of optical electro- and magnetostriction, *Phys. Rev. A* **107**, 023525 (2023).
- [79] G. M. Hale and M. R. Query, Optical constants of water in the 200-nm to 200- μm wavelength region, *Appl. Opt.* **12**, 555 (1973).
- [80] L.-F. Yang and K. J. Webb, Pushing and pulling optical pressure control with plasmonic surface waves, *Phys. Rev. B* **103**, 245124 (2021).
- [81] L. D. Landau and E. M. Lifshitz, *The Classical Theory of Fields*, 4th ed., Course of Theoretical Physics (Pergamon Press, New York, 1975), Vol. 2, Chap. 4, pp. 80–82.
- [82] A. Einstein and J. Laub, On the ponderomotive forces exerted on bodies at rest in the electromagnetic field, in *The Collected Papers of Albert Einstein: The Swiss Years: Writings, 1900–1909. (English Translation Supplement)* (Princeton University Press, Princeton, NJ, 1989), Vol. 2, pp. 339–348, translated to English by Anna Beck.